Aerospace Science and Technology 45 (2015) 294–308

Contents lists available at ScienceDirect

Aerospace Science and Technology

www.elsevier.com/locate/aescte

# A novel nonlinear hybrid controller design for an uncertain quadrotor with disturbances

Alireza Modirrousta, Mahdi Khodabandeh *

*Department of Electrical Engineering, Hamedan University of Technology, Hamedan, 65155, Iran*

ARTICLE INFO

*Article history:*
Received 25 January 2015
Received in revised form 21 April 2015
Accepted 30 May 2015
Available online 3 June 2015

*Keywords:*
Quadrotor
Adaptive control
Terminal sliding mode
Free chattering design
Robust PID

ABSTRACT

In this paper, two adaptive robust nonlinear controllers are proposed. A hybrid controller is developed and applied to a quadrotor to attenuate the chattering effects, and to achieve finite time convergence and robustness aims. Firstly, integral backstepping control is combined with adaptive terminal sliding mode to control the attitude of the quadrotor. The derivative of control signal is obtained from a terminal second-layer sliding surface, and contains the integral of the switching control law. Secondly, an adaptive robust PID controller is designed for the position control of the quadrotor and is improved for free chattering and robust performance against external disturbances. Finally, the adaptive control law is modified for practical applications. The stability and robustness of the proposed controller have been proved using the classic Lyapunov criterion. Then the hybrid controller has been successfully applied on the quadrotor with considering disturbances, noises and uncertainties.



## 1. Introduction

In the past few years, the interest in Unmanned Aerial Vehicle (UAV), especially quadrotors, has been grown strongly. The design of flight controllers which are able to offer UAVs an accurate and robust control is an important part of the fully autonomous vehicles design. Fixed wing UAVs have been used in surveillance and different missions for years, but their lack of stationary flight capability has shifted the focus to vertical Take-Off and Landing (VTOL) vehicles, which are offering ability to hover above a target. The quadrotor is one of the most important VTOL vehicles that can reach a stable hovering and flight using the equilibrium forces produced by four rotors. One of the other important advantages of the quadrotor configuration is its maneuver possibility.

Different control methods have been explored for the attitude and position control of quadrotor. The dynamic model of a quadrotor has been investigated by researchers in [1]. In [2], backstepping and conventional sliding mode control have been developed, which is easy to implement practically. Researchers worked also on backstepping control for quadrotor stabilization in [3]. Integral backstepping has been used in [4,5] to modify the simple backstepping scheme and reduce the steady state error. Sliding mode control has been used for ensuring desired tracking trajectories and eliminating the effects of the perturbations in [6]. Robustness is an important issue in quadrotor flight in outdoor situations. In [7], sliding mode control has been used in the presence of disturbances for robust flight control. Nonlinear disturbance observer has been proposed for quadrotor control in [8] to estimate the disturbance without high gain values and massive computational process. Super twisting algorithm has been applied for quadrotor in [9] in order to ensure robustness against bounded disturbances. But, external disturbances have not been considered in all the outputs of the system at the same time.

Adaptive algorithm is used to online estimation of controller parameters. In [10], adaptive sliding mode control has been used for trajectory tracking considering underground effects and noisy sensors. The combination of backstepping and sliding mode control can be found as an impressive control design, which is used in this paper for attitude control. A method based on adaptive backstepping sliding mode has been proposed in [11] for chaos synchronization with external disturbances. Moreover, an adaptive sliding mode backstepping control has been applied for robot manipulator in [12]. In this design, the results have been compared with a robust neural network based algorithm and its authority has been proved. PD-2 feedback controller has been also applied for the compensation of the Coriolis and gyroscopic torques [13,14]. Direct approximate-adaptive control, using Combined Model Adaptive Control (CMAC) with nonlinear approximation has been presented in [15] and robustness properties to disturbances and unknown payloads have been achieved. In [16], a robust adaptive control scheme has been proposed by using baseline control with model reference adaptive control to acquire the quadrotor motion

* Corresponding author.
*E-mail address:* khodabandeh@hut.ac.ir (M. Khodabandeh).

http://dx.doi.org/10.1016/j.ast.2015.05.022
1270-9638/

control. In addition, a robust adaptive PID has been developed for robot manipulators in [17]. Recently, under actuated sliding mode control scheme has been applied for the quadrotor and details of it can be found in [18]. In that paper, a synthesis control method has been proposed for the robust motion of the quadrotor. But, some control signals are not feasible easily in that design.

In this paper, an innovative control scheme is proposed for robust and finite time convergence of quadrotor attitude. Free chattering robust PID controller is also introduced for the position control. This control algorithm decreases the chattering phenomena and improves transient response, in comparison with the controller proposed in [17]. The main attributes of the designed controller are robustness, finite time stabilization and free chattering control input. Moreover, modified adaptive tuning law is used to estimate the unknown bounded external disturbances. Although, disturbances have not been considered together in all parts of the system in the some researches [6–10], but it is applied in both rotational and translational dynamic in this paper. The main contributions of the work are: first, proposing integral backstepping method which is combined with terminal sliding mode and adaptive control scheme to reach the mentioned aims. Second, modifying the robust PID control based on [17], to achieve a free chattering control signal and robustness. In this design, the new adaptive laws are used for the quadrotor position control. Third, adaptive control law has been modified by using fuzzy factors instead of constant adaptive gains. It has been used to avoid boundless increase of adaptive gains and it can make an appropriate tracking accuracy in the presence of external disturbances. Numerical simulations are achieved to validate the performance of the proposed controller and some comparison studies are presented to show their advantages.

The paper is organized as follows: some necessary assumptions and lemmas are provided in Section 2. In Section 3, a brief description of the system model is given. The proposed controllers for rotational and translational system and their stability analyses are proposed in Sections 4 and 5, respectively. The fuzzy adaptation range factor is designed in Section 6. Simulation results are provided in Section 7. Finally some conclusions are made.

## 2. Assumptions and lemmas

### 2.1. Lemmas

Following lemmas are required for some mathematical aspects of the controller design. They are introduced as follows:

**Lemma 1.** *(See [19].) For $x_i \in \mathbb{R}$, $i = 1, 2, \ldots, n$, $0 < p \le 1$ is a real number, then the following inequality holds:*

$$\left(|x_1| + |x_2| + \cdots + |x_n|\right)^p \le |x_1|^p + \cdots + |x_n|^p \tag{1}$$

**Lemma 2.** *(See [20].) Assume that a continuous, positive definite function $V(t)$ satisfies the following differential inequality:*

$$\dot{V}(t) \le -cV^{\xi}(t) \quad \forall t \le t_0 \quad V(t_0) \ge 0 \tag{2}$$

*where $c > 0$ and $0 < \xi < 1$ are two constants. Then, for any given $t_0$, $V(t)$ satisfies the following inequality:*

$$V^{1-\xi}(t) \le V^{1-\xi}(t_0) - c(1-\xi)(t - t_0), \quad t_0 \le t \le t_1 \tag{3}$$

*and $V(t) \equiv 0$, $\forall t \ge t_1$ with $t_1$ given by:*

$$t_1 = t_0 + \frac{V^{1-\xi}(t_0)}{c(1-\xi)} \tag{4}$$

**Lemma 3.** *(See [21].) For every given scalar $x$ and positive scalar $y$, the following inequality holds:*

$$x\tanh(yx) = \left|x\tanh(yx)\right| = |x|\left|\tanh(yx)\right|$$

### 2.2. Assumptions

The following assumptions are defined for the proposed control system:

**Assumption 1.** All the states of the quadrotor system are measurable.

**Assumption 2.** The external disturbances $\dot{d}_i(t)$ are assumed to be bounded and maximum bounds of them are defined by $D_i$:

$$\left|\frac{d}{dt}(\tau_d)\right| = \left|\dot{d}_i(t)\right| < D_i \quad \text{for } i = 1, 2, 3, 4.$$

**Assumption 3.** The reference inputs for translational motion of the quadrotor and their derivatives are bounded.

**Assumption 4.** External disturbances including wind guest effects, aerodynamic effects and perturbation based on error term are assumed to be bounded by unknown values. Additionally, reference inputs are also bounded and are considered as disturbance from as:

$$|W_i| + |\dot{x}_{(2i)d}| + \Gamma_i|\dot{e}_{2i-1}| + |e_{2i-1}| \le \tau_{i,1} + \tau_{i,2}\|e_T\| + \tau_{i,3}\|\dot{e}_T\| + \tau_{i,4}\left\|\int_0^t e_T dt\right\|$$

where $\Gamma_i$, $W_i$ and $\dot{x}_{(2i)d}$ are positive constant, disturbance effect and reference input, respectively, and are defined later. This assumption is also valid for matched and mismatched uncertainties [22] when there is knowledge about the uncertain terms based on systems states.

## 3. Dynamic model

In this section, the basic state-space model of the quadrotor is described [1]. The dynamics of the four rotors are much faster than the main system and thus, they are neglected in this case. The generalized coordinates of the rotorcraft are $q = (x, y, z, \psi, \theta, \phi)$, where $\xi = (x, y, z) \in \Re^3$ represents the relative position of the rotorcraft with respect to an inertial frame and $\eta = (\psi, \theta, \phi) \in S^3$ are the three Euler angles representing the orientation of the rotorcraft, called yaw, pitch and roll of the vehicle. Considering kinetic and potential energy of the system, let define Lagrangian as $L(q, \dot{q}) = T_{rot} + T_{trans} - u$, where $T_{trans} = \frac{m}{2}\dot{\xi}^T\dot{\xi}$ is the translational kinetic energy, $T_{rot} = \frac{1}{2}\dot{\eta}^T J\dot{\eta}$ is the rotational kinetic energy, $u = mgz$ is the potential energy, $z$ is the quadrotor altitude, $g$ is the acceleration of gravity, $m$ is the mass of quadrotor and $J$ is the auxiliary matrix expressed in terms of $\eta$.

The dynamic of quadrotor is obtained from Euler–Lagrangian equations considering external forces $F = (F_\xi, \tau)$ as follows:

$$\frac{d}{dt}\frac{\partial L}{\partial \dot{q}} - \frac{\partial L}{\partial q} = F \tag{5}$$

Neglecting body forces because of their small amplitude, one get:

$$\hat{F} = \begin{pmatrix} 0 \\ 0 \\ u \end{pmatrix} \tag{6}$$

The main thrust is described as:

$$u = f_1 + f_2 + f_3 + f_4 \tag{7}$$

where $f_i = k_i\omega_i^2$, $i = 1, \ldots, 4$ and $k_i$ are positive constants and $\omega$ is the angular speed of each motor. Then, $F_\xi$ can be rewritten as $F_\xi = R\hat{F}$, where $R$ is translational matrix which can be shown as follows:

$$R = \begin{pmatrix} c\theta c\psi & c\psi s\theta s\phi - s\psi c\phi & c\psi s\theta c\phi + s\psi s\phi \\ s\psi s\theta & s\psi s\theta s\phi + c\psi c\phi & s\psi s\theta c\phi - c\psi s\phi \\ -s\theta & c\theta s\phi & c\theta c\phi \end{pmatrix} \tag{8}$$

where $c$ and $s$ denote cos and sin respectively.

The generalized torque for the $\eta$ variables is defined as:

$$\tau = \begin{pmatrix} \tau_\phi \\ \tau_\theta \\ \tau_\psi \end{pmatrix} \tag{9}$$

where

$$\tau_\psi = \sum_{i=1}^{4} \tau_{M_i}$$
$$\tau_{M_i} = d(f_1 - f_2 + f_3 - f_4)$$
$$\tau_\theta = (f_2 - f_4)l$$
$$\tau_\phi = (f_3 - f_1)l \tag{10}$$

Thus the control distribution from the four actuator motors of the quadrotor is given by:

$$\begin{pmatrix} u \\ \tau_\phi \\ \tau_\theta \\ \tau_\psi \end{pmatrix} = \begin{pmatrix} 1 & 1 & 1 & 1 \\ -l & 0 & l & 0 \\ 0 & l & 0 & -l \\ d & -d & d & -d \end{pmatrix} \begin{pmatrix} f_1 \\ f_2 \\ f_3 \\ f_4 \end{pmatrix} \tag{11}$$

where $l$ is the distance from the motors to the center of gravity and $c$ is a constant known as force-to-moment scaling factor. $d$ and $b$ ($b = k$) have usually been called the coefficient of thrust and yawing moment. Totally, dynamic model of quadrotor can be obtained for the hover flight by the following equations:

$$m\ddot{\xi} + \begin{pmatrix} 0 \\ 0 \\ mg \end{pmatrix} = F_\xi + W \tag{12}$$

$$J\ddot{\eta} + \dot{J}\dot{\eta} - \frac{1}{2}\frac{\delta}{\delta\eta}(\dot{\eta}^T J\dot{\eta}) = \tau + \tau_d$$
$$\overline{V}(\eta, \dot{\eta}) = \dot{J}\dot{\eta} - \frac{1}{2}\frac{\delta}{\delta\eta}(\dot{\eta}^T J\dot{\eta})$$
$$J\ddot{\eta} + \overline{V}(\eta, \dot{\eta}) = \tau$$
$$\overline{V}(\eta, \dot{\eta}) = \left(\dot{J} - \frac{1}{2}\frac{\delta}{\delta\eta}(\dot{\eta}^T J)\right)\dot{\eta} = C(\eta, \dot{\eta})\dot{\eta} \tag{13}$$

where $W$ is the vector of the disturbances that are explained later and $\tau_d = \begin{pmatrix} \tau_\phi^d \\ \tau_\theta^d \\ \tau_\psi^d \end{pmatrix}$ is the disturbance torque vector. By substituting $F_\xi$ with Eq. (12), the state-space of translation motion with external disturbances in $z$-axis can be obtained as follows:

$$\begin{pmatrix} \ddot{x} \\ \ddot{y} \\ \ddot{z} \end{pmatrix} = -\begin{pmatrix} 0 \\ 0 \\ g \end{pmatrix} + \frac{1}{m}\begin{pmatrix} c\psi s\theta c\phi + s\psi s\phi \\ s\psi s\theta c\phi - c\psi s\phi \\ c\theta c\phi \end{pmatrix} u - \begin{pmatrix} \frac{K_1}{m}\dot{x} \\ \frac{K_2}{m}\dot{y} \\ \frac{K_3}{m}\dot{z} \end{pmatrix} + W_i(t) \tag{14}$$

where drag effects are considered in $W_i(t)$. Furthermore, due to the small angles $\psi, \theta, \phi$, the dynamic model of the quadrotor for rotational motion is rewritten as the following form:

$$\begin{pmatrix} \ddot{\phi} \\ \ddot{\theta} \\ \ddot{\psi} \end{pmatrix} = f(\phi, \theta, \psi) + g(\phi, \theta, \psi)\tau - \begin{pmatrix} \frac{K_1 l}{I_x}\dot{\phi} \\ \frac{K_5 l}{I_y}\dot{\theta} \\ \frac{K_6 l}{I_z}\dot{\psi} \end{pmatrix} \tag{15}$$

where

$$f(\phi, \theta, \psi) = \begin{pmatrix} \dot{\theta}\dot{\phi}(\frac{I_y - I_z}{I_x}) - \frac{J_p}{I_x}\dot{\theta}\Omega \\ \dot{\psi}\dot{\phi}(\frac{I_z - I_x}{I_y}) - \frac{J_p}{I_y}\dot{\psi}\Omega \\ \dot{\psi}\dot{\theta}(\frac{I_x - I_y}{I_z}) \end{pmatrix},$$
$$g(\phi, \theta, \psi) = \begin{pmatrix} \frac{l}{I_x} & 0 & 0 \\ 0 & \frac{l}{I_y} & 0 \\ 0 & 0 & \frac{l}{I_z} \end{pmatrix}$$

where $\Omega = \omega_2 + \omega_4 - \omega_1 - \omega_3$, $I_{x,y,z}$ are body inertia, $K_i$ (different from $k_i$ which are designed in the controller design) denote drag coefficients and they are positive constants. $J_p$ is the propeller rotor inertia. To avoid repetition, the state-space model of Euler angles (Roll, Pitch and Yaw) is considered as follows:

$$\dot{x}_{2i-1} = x_{2i}$$
$$\dot{x}_{2i} = f_i(X) + g_i\tau_i + d_i, \quad \text{for } i = 1, \ldots, 3$$
$$y_i = x_{2i-1} \tag{16}$$

where $X = [x_1, x_2, x_3, x_4, x_5, x_6]^T := [\phi, \dot{\phi}, \theta, \dot{\theta}, \psi, \dot{\psi}]^T$ is the system state, $[d_1, d_2, d_3]^T := [\tau_\phi^d, \tau_\theta^d, \tau_\psi^d]^T$ are the disturbances and drag effects, $[g_1, g_2, g_3]^T := [\frac{l}{I_x}, \frac{l}{I_y}, \frac{l}{I_z}]^T$ are the weighting parameters of the control signal, $f_i(X)$ is obtained from the proportionate row according to Eq. (15) and $u_i = \tau_i$ is the control input for each $i$ ($i = 1, 2, 3$). Fig. 1 shows the structure of the quadrotor control.

## 4. Controller design and stability analysis for the rotational system

The aim of developing a sliding mode controller is to achieve robustness against uncertainty, unmodeled dynamic and bounded disturbances. The sliding mode control can be used upon regulatory variables to bring the new variables to the equilibrium state. However, high frequency chattering in the control input is the problem and can cause instability to the system by exciting unmodeled dynamics and even can lead to breakdown. Defining the second layer of sliding mode by terminal sliding mode, makes it possible to obtain the control input by integrating the discontinuous signal of conventional sliding mode. In order to achieve this continuous control signal, integral backstepping method is combined with terminal sliding mode control. Moreover, adaptive method is used to achieve robustness and better response.

First, the whole system dynamic are redefined in terms of some error variables. Defining $e_{2i-1} = x_{2i-1} - x_d$ as error equation, $\dot{\zeta}_{2i-1} = e_{2i-1}$ can be added to error dynamics of the system to improve the tracking accuracy and it are known as an augmented state. The variable $x_d$ is the desired command of each state. Then, the error dynamics of the system can be rewritten as follows:

$$\dot{\zeta}_{2i-1} = e_{2i-1}$$
$$\dot{e}_{2i-1} = e_{2i}$$
$$\dot{e}_{2i} = f_i(e) + g_i\tau_i + d_i, \quad i = 1, 2, 3 \tag{17}$$

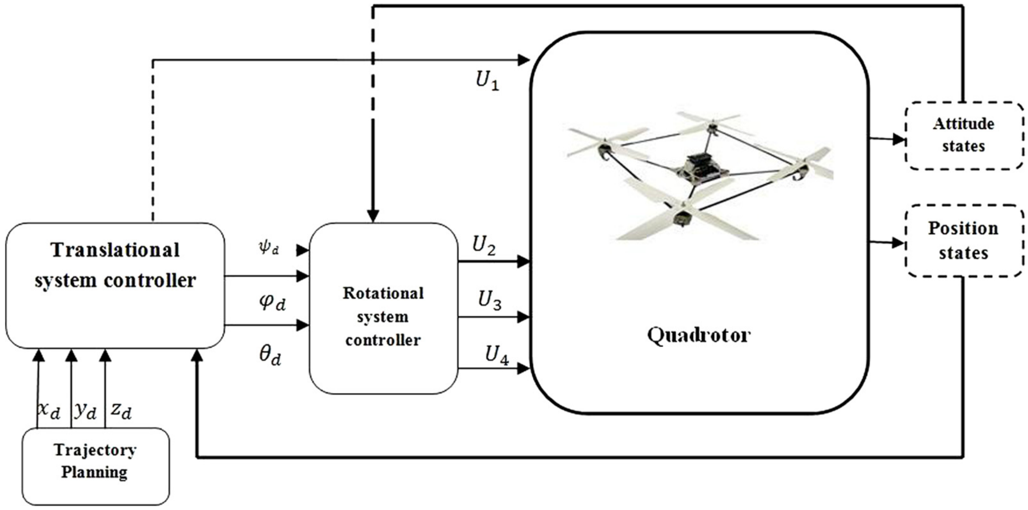


**Fig. 1.** The structure of the two proposed controllers for the quadrotor.

The derivative of the error equation is:

$$\dot{e}_{2i-1} = \dot{x}_{2i-1} - \dot{x}_{(2i-1)d} = x_{2i} - \dot{x}_{(2i-1)d} \tag{18}$$

Let $x_{2i}$ be a virtual input which should be stabilized. Lyapunov candidate is introduced as

$$V_1 = 1/2\sum_{i=1}^{3}(\zeta_{2i-1}^2 + e_{2i-1}^2) \tag{19}$$

The following state feedback control is proposed:

$$x_{2i} = -\zeta_{2i-1} + \dot{x}_{(2i-1)d} - \alpha_i e_{2i-1} \tag{20}$$

where $\alpha_i$ are positive constants. Then, the error of the virtual inputs is defined as $z_{2i-1} = x_{2i} - \mu_i$, where $\mu_i = -\zeta_{2i-1} + \dot{x}_{(2i-1)d} - \alpha_i e_{2i-1}$ and the closed loop system is obtained as $\dot{x}_{2i-1} = z_{2i-1} + \mu_i = z_{2i-1} - \zeta_{2i-1} + \dot{x}_{(2i-1)d} - \alpha_i e_{2i-1}$. Then the derivative of $V_i$ is obtained as below

$$\dot{V}_1 = \sum_{i=1}^{3}(\zeta_{2i-1}.\dot{\zeta}_{2i-1} + e_{2i-1}.\dot{e}_{2i-1})$$

$$\dot{V}_1 = \sum_{i=1}^{3}\big(e_{2i-1}.(\zeta_{2i-1} + x_{2i} - \dot{x}_{(2i-1)d})\big) \tag{21}$$

Substituting Eq. (20) to the derivative of Lyapunov function, yields following:

$$\dot{V}_1 \le -\sum_{i=1}^{3}\alpha_i.e_{2i-1}^2 + z_{2i-1}.e_{2i-1} \tag{22}$$

where the controller design should be modified for global stability.

The proposed controller is based on finite time approach, terminal second order sliding mode and adaptive control. This controller provides the complete compensation of the uncertainty and disturbance for attitude of the quadrotor. Since the virtual control variable and the derived stabilizing function are not equal, thus the first-layer of the sliding surface is defined in terms of virtual variable error and by using integral sliding mode control. Therefore, the convergence of error of virtual input to zero is achieved. Finally, a conventional sliding surface [23] with integral state is defined as follows [24]:

$$s_i = \left(\frac{d}{dt} + \lambda_i\right)^{n-1}\int z_{2i-1} \tag{23}$$

where $n$ is chosen as 2, $\lambda_i$ are positive constants and then, it is obtained as:

$$s_i = z_{2i-1} + \lambda_i \int_o^t z_{2i-1}\,dt \tag{24}$$

The derivative of the sliding surface is calculated as:

$$\dot{s}_i = \dot{z}_{2i-1} + \lambda_i z_{2i-1} \tag{25}$$

and $\dot{z}_{2i-1}$ is obtained as:

$$\dot{z}_{2i-1} = \dot{x}_{2i} - \dot{\mu}_i = f_i(x) + g_i(x)\tau_i + d_i - \dot{\mu}_i$$
$$\dot{z}_{2i-1} = z_{2i} \tag{26}$$

The second sliding surface can be designed based on previous surfaces and its derivative in the form of terminal sliding mode. The terminal sliding surface is chosen as Eq. (27) to guarantee the previous sliding surfaces convergence to zero in finite time and to achieve the second-order sliding mode control [25,26]. In this paper, a second-layer of sliding mode surface is considered as following

$$\sigma_i = \dot{s}_i + \beta_i|s_i|^{\gamma_i}\operatorname{sign}(s_i) \tag{27}$$

where $\beta_i$ are positive constants and $0.5 < \gamma_i < 1$.

Whenever the second-layer sliding surface converges to zero, each integral sliding surface, which has been described by Eq. (24), reaches to zero in finite time [27] as follows:

$$t_{r_i} = \frac{|s_i(0)|^{1-\gamma_i}}{\beta_i(1-\gamma_i)} \tag{28}$$

When the second-layer terminal sliding surface converges to zero, the finite time convergence of integral sliding surface is guaranteed. The derivative of the second-layer is obtained as:

$$\dot{\sigma}_i = \ddot{s}_i + \beta_i\gamma_i|s_i|^{\gamma_i-1}\dot{s}_i \tag{29}$$

where

$$\ddot{s}_i = \dot{z}_{2i} + \lambda_i z_{2i} \tag{30}$$

The proposed controller is designed as following:

$$\tau_i = u_{ei} + u_{si} + u_{ni} \tag{31}$$

where $u_e$ is the equivalent control which is obtained from the derivative of the second terminal sliding surface Eq. (29). $u_s$ is the adaptive switching control which makes the second-layer terminal sliding surface stable in finite time and robust against the external disturbances. $u_n$ is designed to ensure the finite time convergence of tracking errors. Actually, the control input is achieved from integrating discontinuous signal and it attenuates the chattering effect. Control signals are defined based on the model introduced by Eq. (16) as the following:

$$\dot{u}_{ei} = g_i^{-1}(x)\big(-\dot{f}_i(x) - (\dot{g}_i(x).\tau_i) + \ddot{\mu}_i - \lambda_i z_{2i} - \beta_i\gamma_i|s_i|^{\gamma_i-1}\dot{s}_i\big) \tag{32}$$

where $g_i^{-1}(x) \neq 0$ from Eq. (20) and $\dot{g}_i(x)$ are zero for $i = 1, 2, 3$ in terms of constant inertia.

$$u_{si} = -\int g_i^{-1}.\hat{k}_i.\operatorname{sign}(\sigma_i) \tag{33}$$

where $\hat{k}_i$ are the estimates value for $k_i$ where they are the upper bounds of uncertainties or disturbance for $i = 1, 2, 3$. And the error between the estimated values and the real ones are defined as $\tilde{k}_i = \hat{k}_i - k_i$. Estimation laws are:

$$\dot{\hat{k}}_i = \upsilon_i.|\sigma_i| \tag{34}$$

where $0 < \upsilon_i < 1$.

$$u_{ni} = -\big(g_i^{-1}\big)\int \frac{b_T.\sigma_i}{\|\sigma\|^2}dt \tag{35}$$

where $\sigma = [\sigma_1, \sigma_2, \sigma_3]^T$.

$$\begin{aligned} b_T &= \sum_{n=1}^{3}\big(b_1|\zeta_{2n-1}| + b_2|e_{2n-1}|\big) \\ &= b_1\big(|\zeta_1| + |\zeta_3| + |\zeta_5|\big) + b_0\big(|e_1| + |e_3| + |e_5|\big) \\ &\quad + |z_1||e_1| + |z_3||e_3| + |z_5||e_5| \end{aligned} \tag{36}$$

where $b_2 = b_0 + |z_{2n-1}|$.

The proposed control law in Eq. (31) with the adaptation laws in Eq. (34) guarantees time occurrence of sliding motion, which is proved in the following theorem.

**Theorem 1.** *Considering Assumptions 1 and 2, if the system error is controlled with control law Eq. (31) and the adaptation laws in Eq. (34), then all the states of the system, $\zeta_i$, $e_i$ and the previously defined sliding surface $\sigma_i$ moves toward zero in a finite time $T_{ri}$, while it has started in any initial point.*

$$T_{ri} \le \frac{2(\frac{1}{2}(\sum_{i=1}^{4}\zeta_{2i-1}^2(0) + e_{2i-1}^2(0) + \sigma_i^2(0) + \frac{1}{\vartheta_i}(\hat{k}_i(0) - k_i)^2))^{1/2}}{\min(\varepsilon_i\sqrt{2}, \omega_i\sqrt{2\vartheta_i}, b_1\sqrt{2}, b_0\sqrt{2})} \tag{37}$$

**Proof.** Choose a positive definite function in the form of

$$V_2(t) = V_1 + \frac{1}{2}\sum_{i=1}^{3}\left(\sigma_i^2 + \frac{1}{\vartheta_i}\tilde{k}_i^2\right) \tag{38}$$

where $\Gamma_i$ are positive, $\tilde{k}_i = \hat{k}_i - k_i$ are the estimate errors for $i = 1, 2, 3$ and $\dot{k}_i = 0$, because of their slow rate of change. Taking the time derivative of $V_2(t)$,

$$\dot{V}_2(t) = \sum_{i=1}^{3}\left(\dot{\zeta}_{2i-1}\zeta_{2i-1} + e_{2i-1}\dot{e}_{2i-1} + \sigma_i\dot{\sigma}_i + \frac{1}{\vartheta_i}\dot{\hat{k}}_i\tilde{k}_i\right) \tag{39}$$

Substituting $\dot{V}_1$ from Eq. (22) and the adaptation laws Eq. (34) into (39):

$$\begin{aligned} \dot{V}_2(t) &= \sum_{i=1}^{3}\left(-c_i.e_{2i-1}^2 + z_{2i-1}.e_{2i-1} + \sigma_i\dot{\sigma}_i + \frac{1}{\vartheta_i}\upsilon_i.|\sigma_i|.\tilde{k}_i\right) \\ \dot{V}_2(t) &= \sum_{i=1}^{3}\bigg(-c_i.e_{2i-1}^2 + z_{2i-1}.e_{2i-1} + \sigma_i\big(\ddot{s}_i + \beta_i\gamma_i|s_i|^{\gamma_i-1}\dot{s}_i\big) \\ &\quad + \frac{\upsilon_i}{\vartheta_i}.|\sigma_i|.\tilde{k}_i\bigg) \end{aligned} \tag{40}$$

According to Eq. (30), it is obtained as:

$$\begin{aligned} \dot{V}_2(t) &= \sum_{i=1}^{3}\bigg(-c_i.e_{2i-1}^2 + z_{2i-1}.e_{2i-1} \\ &\quad + \sigma_i\big(\dot{z}_{2i} + \lambda_i z_{2i} + \beta_i\gamma_i|s_i|^{\gamma_i-1}\dot{s}_i\big) + \frac{\upsilon_i}{\vartheta_i}.|\sigma_i|.\tilde{k}_i\bigg) \end{aligned} \tag{41}$$

Substituting Eq. (26) and taking derivative, it results the following:

$$\begin{aligned} \dot{V}_2(t) &= \sum_{i=1}^{3}\bigg(-c_i.e_{2i-1}^2 + z_{2i-1}.e_{2i-1} + \sigma_i\big(\dot{f}_i(x) + g_i(x)\dot{\tau}_i + \dot{g}_i\tau_i \\ &\quad + \dot{d}_i - \ddot{\mu}_i + \lambda_i z_{2i} + \beta_i\gamma_i|s_i|^{\gamma_i-1}\dot{s}_i\big) + \frac{\upsilon_i}{\vartheta_i}.|\sigma_i|.\tilde{k}_i\bigg) \end{aligned} \tag{42}$$

Using Assumption 2 and introducing $u_i$,

$$\begin{aligned} \dot{V}_2(t) &\le \sum_{i=1}^{3}\bigg(-c_i.e_{2i-1}^2 + |z_{2i-1}|.|e_{2i-1}| \\ &\quad + \sigma_i\left(-\hat{k}_i.\operatorname{sign}(\sigma_i) - \frac{b_T\sigma_i}{\|\sigma\|^2} + D_i\right) + \frac{\upsilon_i}{\vartheta_i}.|\sigma_i|.\tilde{k}_i\bigg) \\ \dot{V}_2(t) &\le \sum_{i=1}^{3}\bigg(-c_i.e_{2i-1}^2 + |z_{2i-1}|.|e_{2i-1}| + \sigma_i\bigg(-\hat{k}_i.\operatorname{sign}(\sigma_i) \\ &\quad + k_i\operatorname{sign}(\sigma_i) - k\operatorname{sign}(\sigma_i) - \frac{b_T\sigma_i}{\|\sigma\|^2} + D_i\bigg) \\ &\quad + \frac{\upsilon_i}{\vartheta_i}.|\sigma_i|.\tilde{k}_i\bigg) \end{aligned} \tag{43}$$

Using the fact that $\sum_{i=1}^{3}\sigma_i(\frac{\sigma_i}{\|\sigma\|^2}) = 1$ and $-\hat{k}_i\operatorname{sign}(\sigma_i) + k_i\operatorname{sign}(\sigma_i) = -\tilde{k}_i\operatorname{sign}(\sigma_i)$, it is obtained that:

$$\begin{aligned} \dot{V}_2(t) &\le \sum_{i=1}^{3}\bigg(-c_i.e_{2i-1}^2 + |z_{2i-1}|.|e_{2i-1}| + \sigma_i\bigg(-\tilde{k}_i\operatorname{sign}(\sigma_i) \\ &\quad - k_i\operatorname{sign}(\sigma_i) - \frac{b_T\sigma_i}{\|\sigma\|^2}\bigg) + |\sigma_i|D_i + \frac{\upsilon_i}{\vartheta_i}.|\sigma_i|.\tilde{k}_i\bigg) \\ \dot{V}_2(t) &\le \sum_{i=1}^{3}\bigg(|z_{2i-1}|.|e_{2i-1}| - \tilde{k}_i|\sigma_i| \\ &\quad - k_i|\sigma_i| + |\sigma_i|D_i - b_T + \frac{\upsilon_i}{\vartheta_i}.|\sigma_i|.\tilde{k}_i\bigg) \\ \dot{V}_2(t) &\le \sum_{i=1}^{3}\bigg(|z_{2i-1}|.|e_{2i-1}| \\ &\quad - (k_i - D_i)|\sigma_i| + \tilde{k}_i\left(-|\sigma_i| + \frac{\upsilon_i}{\vartheta_i}.|\sigma_i|\right) - b_T\bigg) \end{aligned} \tag{44}$$

It yields:

$$\dot{V}_2(t) \le \sum_{i=1}^{3}\Big(-(k_i - D_i)|\sigma_i| - \Big(|\sigma_i| - \frac{\upsilon_i}{\vartheta_i}.|\sigma_i|\Big).\tilde{k}_i - \big(b_1|\zeta_{2i-1}| + b_0|e_{2i-1}|\big)\Big) \tag{45}$$

Therefore, there always exists $k_i$ and $\vartheta_i$ such that $k_i > D_i$ and $\vartheta_i > \upsilon_i$ [28], which yields $\varepsilon_i > 0$ and $\omega_i > 0$. Where they are defined as $\varepsilon_i = k_i - D_i$ and $\omega_i = |\sigma_i| - \frac{\upsilon_i}{\vartheta_i}.|\sigma_i|$. Then, it is obtained as:

$$\dot{V}_2(t) \le \sum_{i=1}^{3}\big(-\varepsilon_i|\sigma_i| - \omega_i.|\tilde{k}_i| - b_1|\zeta_i| - b_0|e_i|\big)$$

$$\dot{V}_2(t) \le \sum_{i=1}^{3}\Big(-\varepsilon_i.\sqrt{2}\frac{|\sigma_i|}{\sqrt{2}} - \omega_i.\sqrt{2\vartheta_i}\frac{|\tilde{k}_i|}{\sqrt{2\vartheta_i}} - b_1\sqrt{2}\frac{|\zeta_{2i-1}|}{\sqrt{2}} - b_0\sqrt{2}\frac{|e_{2i-1}|}{\sqrt{2}}\Big) \tag{46}$$

And finally:

$$\dot{V}_2(t) \le -\min(\varepsilon_i\sqrt{2}, \omega_i\sqrt{2\vartheta_i}, b_1\sqrt{2}, b_0\sqrt{2}) \times \sum_{i=1}^{3}\Big(\frac{|\sigma_i|}{\sqrt{2}} + \frac{|\tilde{k}_i|}{\sqrt{2\vartheta_i}} + \frac{|\zeta_{2i-1}|}{\sqrt{2}} + \frac{|e_{2i-1}|}{\sqrt{2}}\Big)$$

$$\dot{V}_2(t) \le -\min(\varepsilon_i\sqrt{2}, \omega_i\sqrt{2\vartheta_i}, b_1\sqrt{2}, b_0\sqrt{2}).V_2^{1/2} \tag{47}$$

Therefore, from Lemma 2, the error trajectory $e_{2i-1}(t)$ and the integral error $\zeta_i(t)$ converges to zero and the errors of virtual control converges to the second order sliding surface $\sigma_i(t) = 0$ in the finite time

$$T_{ri} \le \frac{2(\frac{1}{2}(\sum_{i=1}^{4}\zeta_{2i-1}^2(0) + e_{2i-1}^2(0) + \sigma_i^2(0) + \frac{1}{\vartheta_i}(\hat{k}_i(0) - k_i)^2))^{1/2}}{\min(\varepsilon_i\sqrt{2}, \omega_i\sqrt{2\vartheta_i}, b_1\sqrt{2}, b_0\sqrt{2})}.$$

When the second terminal sliding surface converges to zero, virtual control variable converges to the integral sliding surface $s_i(t) = 0$ in finite time ($t_{ri}$).

**Remark 1.** It can be seen in Eqs. (29) and (32) that there are singular points which can cause singularity problem. In order to solve this problem and the unbounded signals, different situations have been analyzed. One of them is occurred when $s_i(t) \ne 0$, $\dot{s}_i(t) \ne 0$, where there is no singular points in it with the proposed design. When the linear surfaces are in the terminal sliding mode, $\sigma_i(t)$ is equal to zero. Then, it leads to $\dot{s}_i = -\beta_i|s_i|^{\gamma_i}\operatorname{sign}(s_i)$ and the term changes to $|s_i|^{\gamma_i-1}\dot{s}_i = -|s_i|^{\gamma_i-1}.\beta_i|s_i|^{\gamma_i}\operatorname{sign}(s_i)$ and $-\beta_i|s_i|^{2\gamma_i-1}\operatorname{sign}(s_i)$; and it can be seen that if $0.5 < \gamma_i < 1$, this term will be nonsingular. But, if $\sigma_i(t)$ is not exactly zero and $s_i(t) = 0$, then there are singular points in the controller and the time derivative of the terminal sliding surface. Thus, the following equations are used to avoid singularity [26,27] and [29]:

$$\dot{\bar{s}}_i = \begin{cases} |s_i|^{\gamma_i-1}\dot{s}_i, & \text{if } s_i(t) \ne 0 \text{ and } \dot{s}_i(t) \ne 0 \\ |\varepsilon_i|^{\gamma_i-1}\dot{s}_i, & \text{if } s_i(t) = 0 \text{ and } \dot{s}_i(t) \ne 0 \\ 0 & \text{if } s_i(t) = 0 \text{ and } \dot{s}_i(t) = 0 \end{cases} \tag{48}$$

where $\varepsilon_i$ are positive small constants. It implies that the improved controller design have no singular points. The redefined Eq. (48) is used in the controller and in the time derivative of terminal sliding surface design. Eq. (29) is rewritten as follows:

$$\dot{\sigma}_i(t) = \ddot{s}_i(t) + \dot{\bar{s}}_i \tag{49}$$

There are some other ways to avoid the singularity, in [30] two linear and nonlinear surfaces have been defined. In this method, linear surface is alternated with nonlinear one while singularity situation happens. In [31], the nonlinear term of sliding surface has been changed and it has been called NTSMC. A saturation function has been used to overcome the singularity in TSMC in [32].

**Remark 2.** The control inputs can be obtained from Eq. (31) with some small angle approximation as following:

$$\tau_\phi = \frac{I_x}{l}\Big(-\dot{\theta}\dot{\phi}\Big(\frac{I_y - I_z}{I_x}\Big) + \frac{J_p}{I_x}\dot{\theta}\Omega + e_\phi - \ddot{\phi}_d + \alpha_1\dot{e}_\phi - \lambda_1 z_\phi - \beta_1\gamma_1\int_0^T \dot{\bar{s}}_1(t)dt - \int_0^T \hat{k}_1(t)\operatorname{sign}\big(\sigma_1(t)\big)dt - \int_0^T \frac{(b_1|\zeta_\phi| + b_2|e_\phi|).\sigma_1(t)}{\|\sigma\|^2}dt\Big) \tag{50}$$

where $e_\phi = e_1 = \phi - \phi_d$ and $\dot{\zeta}_\phi = e_\phi$. The control signals for other Euler angles are obtained the same as the above equations and

$$\tau_\theta = \frac{I_y}{l}\Big(-\dot{\psi}\dot{\phi}\Big(\frac{I_z - I_x}{I_y}\Big) + \frac{J_p}{I_y}\dot{\psi}\Omega + e_\theta - \ddot{\theta}_d + \alpha_2\dot{e}_\theta - \lambda_2 z_\theta - \beta_2\gamma_2\int_0^T \dot{\bar{s}}_2(t)dt - \int_0^T \hat{k}_2(t)\operatorname{sign}\big(\sigma_2(t)\big)dt - \int_0^T \frac{(b_1|\zeta_\theta| + b_2|e_\theta|).\sigma_2(t)}{\|\sigma\|^2}dt\Big) \tag{51}$$

$$\tau_\psi = \frac{I_z}{l}\Big(-\dot{\psi}\dot{\theta}\Big(\frac{I_x - I_y}{I_z}\Big) + e_\psi - \ddot{\psi}_d + \alpha_3\dot{e}_\psi - \lambda_3 z_\psi - \beta_3\gamma_3\int_0^T \dot{\bar{s}}_3(t)dt - \int_0^T \hat{k}_3(t)\operatorname{sign}\big(\sigma_3(t)\big)dt - \int_0^T \frac{(b_1|\zeta_\psi| + b_2|e_\psi|).\sigma_3(t)}{\|\sigma\|^2}dt\Big) \tag{52}$$

**Remark 3.** Hence, the control signal Eq. (35) may increase boundlessly; the following dead-zone technique is used to overcome this difficulty

$$u_{ni} = \begin{cases} -\int \frac{b_T\sigma_i}{\|\sigma\|^2}dt, & |e_{2i-1}| > \epsilon \\ 0, & |e_{2i-1}| < \epsilon \end{cases} \tag{53}$$

where $\epsilon$ is a small positive constant and stability conditions holds in both situations, but finite time convergence is bounded in the domain of $|e_{2i-1}| < \epsilon$.

## 5. Controller design and stability analysis for translational system

In this section, an adaptive robust PID controller is applied for the quadrotor position control. Following equations are used for the translational motion of quadrotor from Eq. (12):

$$\ddot{x} = \frac{u_1}{m}(\cos\psi\sin\theta\cos\phi + \sin\psi\sin\phi) + W_4$$

$$\ddot{y} = \frac{u_1}{m}(\sin\psi\sin\theta\cos\phi - \cos\psi\sin\phi) + W_5$$

$$\ddot{z} = \frac{u_1}{m}(\cos\theta\cos\phi) - g + W_6 \tag{54}$$

where $W_i$, $i = 4, 5, 6$, represent the effect of the wind guests on the quadrotor translational accelerations, aerodynamics and drag effect and other external disturbances. The virtual control input which can be defined for translational system is a function of the thrust and Euler angles, and can be described by the following equations:

$$\cos\psi \sin\theta \cos\phi + \sin\psi \sin\phi = \frac{m}{u_1} U_4$$
$$\sin\psi \sin\theta \cos\phi - \cos\psi \sin\phi = \frac{m}{u_1} U_5$$
$$(\cos\theta \cos\phi) = \frac{m}{u_1} U_6 \tag{55}$$

where $U_i$, $i = 4, 5, 6$ are the virtual control inputs to control the translational motion of the quadrotor. Furthermore, $g$ has been considered as the disturbance and is not appeared in Eq. (55). Based on Theorem 1, there is a small time like $T$, during which, $\theta$, $\psi$ and $\phi$ converge to their equilibrium points and $\tilde{\theta}$, $\tilde{\psi}$ and $\tilde{\phi}$ become zero. Command (desired) states for rotational system are defined by solving Eq. (55). They are achieved as:

$$u_1 = \frac{m}{\cos\theta \cos\phi}(U_6)$$
$$\phi_c = \sin^{-1}\left(\frac{m}{u_1} U_4 \sin\psi - \frac{m}{u_1} U_5 \cos\psi\right)$$
$$\theta_c = \sin^{-1}\left(\frac{m}{u_1} U_4 \cos\psi + \frac{m}{u_1} U_5 \sin\psi\right)$$
$$\psi_c = \psi \tag{56}$$

Translational errors between the reference path and the quadrotor path are defined as $e_7 = x - x_d$, $e_9 = y - y_d$ and $e_{11} = z - z_d$. Finally, the error dynamics of the quadrotor position is described as follows:

$$\dot{e}_{2i-1} = e_{2i}$$
$$\dot{e}_{2i} = U_i + g_i + W_i - \dot{x}_{(2i)d}, \quad i = 4, 5, 6 \tag{57}$$

where $g_4 = 0$, $g_5 = 0$, $g_6 = -g$ are the related terms of $g_i$, $\dot{x}_{(2i)d}$, $i = 4, 5, 6$ are reference acceleration of quadrotor motion around $x$, $y$ and $z$ axis, respectively and $\dot{x}_d$, $\dot{y}_d$ and $\dot{z}_d$ show the desired velocity of the reference path.

In this section, an adaptive robust PID controller is proposed to stabilize the translational motion of the quadrotor in the presence of external disturbances and other defined perturbations. First, auxiliary variables are introduced as:

$$X_i = \dot{e}_{2i-1} + \Gamma_i e_{2i-1} + \int_o^t e_{2i-1} dt \tag{58}$$

where $\Gamma_{2i-1}$ are positive constants. Derivative and integral of the quadrotor position error are also involved in these variables. It is assumed that the upper bound of external disturbance is unknown and a set of estimation laws is considered to deal with these unknown perturbations. The controller should force the position and the velocity tracking errors converge asymptotically to zero. The control signal produced in this section for position control is used as desired or command state in the attitude controller. Therefore a continuous or smooth control signal should be developed for a suitable design. The controller can be designed as follows:

$$U_i = -k_i^P e_{2i-1} - k_i^D \dot{e}_{2i-1} - k_i^I \int_0^t e_{2i-1} dt - \hat{g}_i - u_i^{switching} \tag{59}$$

where $k_i^P$, $k_i^D$ and $k_i^I$ are positive constants and $[\hat{g}_4, \hat{g}_5, \hat{g}_6]^T := [0, 0, \hat{g}]^T$ is the estimate of the gravity effects. The upper bound of the external disturbances cannot be determined easily in real environment and it is estimated by an adaptation laws. Therefore, to guarantee the convergence of auxiliary variables and tracking errors to zero and also to attenuate the chattering phenomenon which traditionally occurs in switching control, the augmented adaptive switching control for PID controller is defined as:

$$u_i^{switching} = \left(\hat{\tau}_{i,1} + \hat{\tau}_{i,2}\|e_T\| + \hat{\tau}_{i,3}\|\dot{e}_T\| + \hat{\tau}_{i,4}\left\|\int_0^t e_T dt\right\|\right)\tanh(X_i) \tag{60}$$

where $e_T = [e_7, e_9, e_{11}]^T$ and $\hat{\tau}_{i,n}$, $n = 1, 2, 3, 4$ are adaptive parameters to undertake and deal with the unknown perturbation and external disturbances based on Assumptions 3 and 4. Therefore, an adaptive tuning law is proposed to estimate the upper bound of $W(t, x)$ and other defined disturbances. When the bounded uncertainty or external disturbances do not exist, the adaptive parameters in Eq. (60) change to adaptation coefficients, which tune the gain and steepness of the tanh function. Adaptation laws can be defined as follows:

$$\dot{\hat{g}}_i = \rho_i |X_i|, \qquad \hat{g}_i(0) = 0$$
$$\dot{\hat{\tau}}_{i,1} = -\rho_i |X_i|, \qquad \hat{\tau}_{i,1}(0) > 0$$
$$\dot{\hat{\tau}}_{i,2} = -\rho_i |X_i| \|e_T\|, \qquad \hat{\tau}_{i,2}(0) > 0$$
$$\dot{\hat{\tau}}_{i,3} = -\rho_i |X_i| \|\dot{e}_T\|, \qquad \hat{\tau}_{i,3}(0) > 0$$
$$\dot{\hat{\tau}}_{i,4} = -\rho_i |X_i| \left\|\int_0^t e_T dt\right\|, \qquad \hat{\tau}_{i,4}(0) > 0 \tag{61}$$

where $\rho_i$ are positive constants and $\hat{\tau}_{i,n}(0)$ are the initial values of the adaptation parameters $\hat{\tau}_{i,n}$, respectively.

**Theorem 2.** *Consider the tracking error system Eq. (57), the continuous control law Eq. (59) and the adaptation laws in Eq. (61), all the error states converges to their zero equilibrium while the following condition is satisfied:*

$$k_i^D = k_i^I$$

**Proof.** Consider the Lyapunov function candidate as:

$$V = \frac{1}{2}\left(\sum_{i=4,5,6} \rho_i X_i^2 + \Omega_{i,1} \sum_{i=4,5,6} e_{2i-1}^2 + \Omega_{i,2} \sum_{i=4,5,6} \left(\int_0^t e_{2i-1} dt\right)^2 + \sum_{i=4,5,6} (\tilde{\tau}_{i,1})^2 + \sum_{i=4,5,6} (\tilde{\tau}_{i,2})^2 + \sum_{i=4,5,6} (\tilde{\tau}_{i,3})^2 + \sum_{i=4,5,6} (\tilde{\tau}_{i,4})^2 + \sum_{i=4,5,6} (\tilde{g}_i)^2\right)$$

where $\Omega_{i,1}$ and $\Omega_{i,2}$ are positive constants that are exactly defined later and $\tilde{\tau}_{i,n} = \hat{\tau}_{i,n} + \tau_{i,n}$, $n = 1, 2, 3, 4$.

Taking derivative of the Lyapunov function candidate with respect to time,

$$\dot{V}=\sum_{i=4,5,6}\Bigg[\rho_i X_i\dot{X}_i+\Omega_{i,1}e_{2i-1}\dot{e}_{2i-1}+\Omega_{i,2}e_{2i-1}\int_0^t e_{2i-1}dt+\dot{\hat{\tau}}_{i,1}(\hat{\tau}_{i,1}+\tau_{i,1})+\dot{\hat{\tau}}_{i,2}(\hat{\tau}_{i,2}+\tau_{i,2})+\dot{\hat{\tau}}_{i,3}(\hat{\tau}_{i,3}+\tau_{i,3})+\dot{\hat{\tau}}_{i,4}(\hat{\tau}_{i,4}+\tau_{i,4})+\dot{\hat{g}}_i\tilde{g}_i\Bigg] \tag{62}$$

Using error dynamic Eq. (57) gives:

$$\dot{V}=\sum_{i=4,5,6}\Bigg[\rho_i X_i(U_i+W_i-g_i-\dot{x}_{(2i)d}+\Gamma_i\dot{e}_{2i-1}+e_{2i-1})+\Omega_{i,1}e_{2i-1}\dot{e}_{2i-1}+\Omega_{i,2}e_{2i-1}\int_0^t e_{2i-1}dt+\dot{\hat{\tau}}_{i,1}(\hat{\tau}_{i,1}+\tau_{i,1})+\dot{\hat{\tau}}_{i,2}(\hat{\tau}_{i,2}+\tau_{i,2})+\dot{\hat{\tau}}_{i,3}(\hat{\tau}_{i,3}+\tau_{i,3})+\dot{\hat{\tau}}_{i,4}(\hat{\tau}_{i,4}+\tau_{i,4})+\dot{\hat{g}}_i\tilde{g}_i\Bigg] \tag{63}$$

Introducing the control law into Eq. (63), the following equation is obtained:

$$\dot{V}=\sum_{i=4,5,6}\Bigg[\rho_i X_i\Bigg(-(k_i^P)e_{2i-1}-k_i^D\dot{e}_{2i-1}+\Gamma_i\dot{e}_{2i-1}+e_{2i-1}-k_i^I\int_0^t e_{2i-1}dt-u_i^{switching}+W_i-\tilde{g}_i-\dot{x}_{(2i)d}\Bigg)+\Omega_{i,1}e_{2i-1}\dot{e}_{2i-1}+\Omega_{i,2}e_{2i-1}\int_0^t e_{2i-1}dt+\dot{\hat{\tau}}_{i,1}(\hat{\tau}_{i,1}+\tau_{i,1})+\dot{\hat{\tau}}_{i,2}(\hat{\tau}_{i,2}+\tau_{i,2})+\dot{\hat{\tau}}_{i,3}(\hat{\tau}_{i,3}+\tau_{i,3})+\dot{\hat{\tau}}_{i,4}(\hat{\tau}_{i,4}+\tau_{i,4})+\dot{\hat{g}}_i\tilde{g}_i\Bigg] \tag{64}$$

The terms $d_i=W_i-\dot{x}_{(2i)d}+\Gamma_i\dot{e}_{2i-1}+e_{2i-1}$ are considered as external disturbances and also Assumption 4 holds. firstly, to avoid repetition, the following equation is considered based on Eq. (64):

$$\dot{V}_1=\sum_{i=4,5,6}\rho_i\Bigg[\Bigg(\dot{e}_{2i-1}+\Gamma_i e_{2i-1}+\int_0^t e_{2i-1}dt\Bigg)\times\Bigg(-k_i^P e_{2i-1}-k_i^D\dot{e}_{2i-1}-k_i^I\int_0^t e_{2i-1}dt\Bigg)+\Omega_{i,1}e_{2i-1}\dot{e}_{2i-1}+\Omega_{i,2}e_{2i-1}\int_0^t e_{2i-1}dt\Bigg]$$

$$\dot{V}_1=\sum_{i=4,5,6}-\rho_i\big(k_i^P+\Gamma_i k_i^D-\Omega_{i,1}\big)e_{2i-1}\dot{e}_{2i-1}-\rho_i k_i^D\dot{e}_{2i-1}^2-\rho_i\big(k_i^D+k_i^I\big)\dot{e}_{2i-1}\int_0^t e_{2i-1}dt-\rho_i\big(k_i^I\Gamma_i+k_i^P-\Omega_{i,2}\big)e_{2i-1}\int_0^t e_{2i-1}dt-\rho_i k_i^I\Bigg(\int_0^t e_{2i-1}dt\Bigg)^2-\rho_i\Gamma_i\big(k_i^P\big)e_{2i-1}^2 \tag{65}$$

Using the fact that $\pm ab\le a^2+b^2$, one get:

$$-\rho_i\big(k_i^D+k_i^I\big)\dot{e}_{2i-1}\int_0^t e_{2i-1}dt\le\frac{1}{2}\rho_i\big(k_i^D+k_i^I\big)\Bigg(\dot{e}_{2i-1}^2+\Bigg(\int_0^t e_{2i-1}dt\Bigg)^2\Bigg)$$

and by introducing $\Omega_{i,1}=k_i^P+\Gamma_i k_i^D$ and $\Omega_{i,2}=k_i^I\Gamma_i+k_i^P$, simplify Eq. (65) to the following:

$$\dot{V}_1=\sum_{i=4,5,6}-\rho_i k_i^D\dot{e}_{2i-1}^2+\frac{1}{2}\rho_i\big(k_i^D+k_i^I\big)\Bigg(\dot{e}_{2i-1}^2+\Bigg(\int_0^t e_{2i-1}dt\Bigg)^2\Bigg)-\rho_i k_i^I\Bigg(\int_0^t e_{2i-1}dt\Bigg)^2-\rho_i\Gamma_i\big(k_i^P\big)e_{2i-1}^2$$

using

$$k_i^D=k_i^I \tag{66}$$

$$\dot{V}_1=\sum_{i=4,5,6}-\rho_i\Gamma_i\big(k_i^P\big)e_{2i-1}^2 \tag{67}$$

Now, on the other terms of the Lyapunov function:

$$\dot{V}_2=\sum_{i=4,5,6}\big[\rho_i X_i\big(d_i-\tilde{g}_i-u_i^{switching}\big)+\dot{\hat{\tau}}_{i,1}(\hat{\tau}_{i,1}+\tau_{i,1})+\dot{\hat{\tau}}_{i,2}(\hat{\tau}_{i,2}+\tau_{i,2})+\dot{\hat{\tau}}_{i,3}(\hat{\tau}_{i,3}+\tau_{i,3})+\dot{\hat{\tau}}_{i,4}(\hat{\tau}_{i,4}+\tau_{i,4})+\dot{\hat{g}}_i\tilde{g}_i\big] \tag{68}$$

According to the adaptation laws and the proposed continuous switching control with Eq. (60):

$$\dot{V}_2=\sum_{i=4,5,6}\Bigg[\rho_i X_i\Bigg(d_i-\Bigg(\hat{\tau}_{i,1}+\hat{\tau}_{i,2}\|e_T\|+\hat{\tau}_{i,3}\|\dot{e}_T\|+\hat{\tau}_{i,4}\Bigg\|\int_0^t e_T dt\Bigg\|\Bigg)\tanh(X_i)\Bigg)-\rho_i|X_i|(\hat{\tau}_{i,1}+\tau_{i,1})-\rho_i|X_i|\|e_T\|(\hat{\tau}_{i,2}+\tau_{i,2})-\rho_i|X_i|\|\dot{e}_T\|(\hat{\tau}_{i,3}+\tau_{i,3})-\rho_i|X_i|\Bigg\|\int_0^t e_T dt\Bigg\|(\hat{\tau}_{i,4}+\tau_{i,4})\Bigg] \tag{69}$$

Using Assumptions 3 and 4:

$$\dot{V}_2 \le \sum_{i=4,5,6}\Bigg[\rho_i X_i\Bigg(\tau_{i,1}+\tau_{i,2}\|e_T\|+\tau_{i,3}\|\dot{e}_T\|+\tau_{i,4}\Bigg\|\int_0^t e_T dt\Bigg\| - \Bigg(\hat{\tau}_{i,1}+\hat{\tau}_{i,2}\|e_T\|+\hat{\tau}_{i,3}\|\dot{e}_T\|+\hat{\tau}_{i,4}\Bigg\|\int_0^t e_T dt\Bigg\|\Bigg)\tanh(X_i)\Bigg) - \rho_i|X_i|(\hat{\tau}_{i,1}+\tau_{i,1}) - \rho_i|X_i|\|e_T\|(\hat{\tau}_{i,2}+\tau_{i,2}) - \rho_i|X_i|\|\dot{e}_T\|(\hat{\tau}_{i,3}+\tau_{i,3}) - \rho_i|X_i|\Bigg\|\int_0^t e_T dt\Bigg\|(\hat{\tau}_{i,4}+\tau_{i,4})\Bigg] \tag{70}$$

It is clear that:

$$\dot{V}_2 \le \sum_{i=4,5,6}\Bigg[\rho_i |X_i|\Bigg(\tau_{i,1}+\tau_{i,2}\|e_T\|+\tau_{i,3}\|\dot{e}_T\|+\tau_{i,4}\Bigg\|\int_0^t e_T dt\Bigg\|\Bigg) - \rho_i X_i\Bigg(\hat{\tau}_{i,1}+\hat{\tau}_{i,2}\|e_T\|+\hat{\tau}_{i,3}\|\dot{e}_T\|+\hat{\tau}_{i,4}\Bigg\|\int_0^t e_T dt\Bigg\|\Bigg) \times\tanh(X_i) - \rho_i|X_i|(\hat{\tau}_{i,1}+\tau_{i,1}) - \rho_i|X_i|\|e_T\|(\hat{\tau}_{i,2}+\tau_{i,2}) - \rho_i|X_i|\|\dot{e}_T\|(\hat{\tau}_{i,3}+\tau_{i,3}) - \rho_i|X_i|\Bigg\|\int_0^t e_T dt\Bigg\|(\hat{\tau}_{i,4}+\tau_{i,4})\Bigg] \tag{71}$$

and

$$\dot{V}_2 \le \sum_{i=4,5,6}\Bigg[-\rho_i X_i\Bigg(\hat{\tau}_{i,1}+\hat{\tau}_{i,2}\|e_T\|+\hat{\tau}_{i,3}\|\dot{e}_T\| + \hat{\tau}_{i,4}\Bigg\|\int_0^t e_T dt\Bigg\|\Bigg)\tanh(X_i) - \rho_i|X_i|(\hat{\tau}_{i,1}) - \rho_i|X_i|\|e_T\|(\hat{\tau}_{i,2}) - \rho_i|X_i|\|\dot{e}_T\|(\hat{\tau}_{i,3}) - \rho_i|X_i|\Bigg\|\int_0^t e_T dt\Bigg\|(\hat{\tau}_{i,4})\Bigg] \tag{72}$$

From Lemma 3, it can be concluded that:

$$\dot{V}_2 \le -\sum_{i=4,5,6}\Bigg[\rho_i |X_i|\Bigg(\hat{\tau}_{i,1}+\hat{\tau}_{i,2}\|e_T\|+\hat{\tau}_{i,3}\|\dot{e}_T\| + \hat{\tau}_{i,4}\Bigg\|\int_0^t e_T dt\Bigg\|\Bigg)\big(\big|\tanh(X_i)\big|+1\big)\Bigg] \tag{73}$$

It is clear that $\hat{\tau}_{i,1}$, $\hat{\tau}_{i,2}$, $\hat{\tau}_{i,3}$ and $\hat{\tau}_{i,4}$ are positive. Eq. (65) can be rewritten as:

$$\dot{V}_2 \le -\sum_{i=4,5,6}\big[G_i|X_i|\big] \tag{74}$$

where $G_i > 0$, $i = 4, 5, 6$. Finally, using Eqs. (67) and (74), the total Lyapunov inequality can be described as follows:

$$\dot{V} = \dot{V}_1 + \dot{V}_2 \le -\sum_{i=4,5,6}\big[\rho_i \Gamma_i(k_i^P)e_{2i-1}^2 + G_i|X_i|\big]$$

Therefore:

$$\dot{V} = -\complement(t) \le 0 \tag{75}$$

where $\complement(t) = \sum_{i=4,5,6}[\rho_i \Gamma_i(k_i^P)e_{2i-1}^2 + G_i|X_i|] \ge 0$ is introduced as an auxiliary variable, and it is uniformly continuous. Integrating Eq. (75) from zero to $t$ yields:

$$\int_0^t \dot{V}d\tau \le -\int_0^t \complement(\tau)d\tau$$

$$V(0) \ge V(t) + \int_0^t \complement(\tau)d\tau$$

$$V(0) \ge \int_0^t \complement(\tau)d\tau \tag{76}$$

Taking the limits as $t \to \infty$ on both sides of Eq. (76) gives:

$$\lim_{t\to\infty}\int_0^t \complement(\tau)d\tau < V(0) < \infty$$

Employing Barbalat Lemma in [19], one can conclude that $\lim_{t\to\infty}\complement(t) = 0$, which implies that $\lim_{t\to\infty}\sum_{i=4,5,6}E = 0$ and $\lim_{t\to\infty}\sum_{i=4,5,6}|X_i| = 0$. So, the designed controller can guarantee that the equilibrium $(\int e, e, \dot{e}, X) = (0, 0, 0, 0)$ is globally and asymptotically stable.

## 6. Fuzzy adaptation range design

In this section, a fuzzy monitoring factor is proposed instead of a constant adaptation range, in order to improve the ability of adaptive control gains. Since practically, $|X_i|$ and $|s_i|$ cannot become exactly zero in finite time, and the adaptive parameters may increase boundlessly, the fuzzy adaptation range is proposed. Actually, in order to avoid overestimation, the proposed adaptation law increases the slope of adaptive parameters whenever sliding surfaces are far from their equilibrium. The slope becomes zero whenever the sliding manifold and tracking errors reach to zero in the presence of external disturbances. The fuzzy factor $\Theta_i$ changes the adaptation range based on the above analysis. The fuzzy control rules can be represented as the mapping of input linguistic variable $s$ and $X$ as follows:

$$\Theta_i = \upsilon_i = F(s_i), \quad \text{for } i = 1, 2, 3$$

$$\Theta_i = \rho_i = F(X_i), \quad \text{for } i = 4, 5, 6$$

where $0 \le \Theta_i \le 1$. The membership functions of the input linguistic for both variables $X_i$ and $s_i$, and the membership functions of the output linguistic variable $\mu_i$, for $i = 1, 2, 3, 4, 5, 6$ are shown in Fig. 2 respectively. These membership functions are used to tune adaptive ranges in position and altitude control. They are also used with different center points for the attitude controller.

The control rules can be defined as follows:

- Rule 1: If $S(X)$ is SNZ Then $\mu$ is M
- Rule 2: If $S(X)$ is BNZ Then $\mu$ is B
- Rule 3: If $S(X)$ is Z Then $\mu$ is Z

where M, B and Z denote the medium, big and zero fuzzy sets of output variable, respectively. SNZ, BNZ and Z show the fuzzy sets of input variable based on the small negative zero, big negative zero and zero, respectively. The rules and membership functions of the input linguistic modify the adaptation slope until the sliding manifold reaches acceptable ranges and avoid growing boundlessly. When the manifold is very far from the zero, the slope chooses the maximum possible value.

## 7. Simulation results

In this section, numerical simulations of the developed strategy are carried out to demonstrate the effectiveness of the proposed adaptive robust control scheme. The dynamic parameters of the model are shown in Table 1 and design parameters are defined as follows:

$$\begin{aligned}
&\beta_1 = 2, \quad \beta_2 = 2, \quad \beta_3 = 2,\\
&\gamma_1 = 3/5, \quad \gamma_2 = 3/5, \quad \gamma_3 = 3/5,\\
&\epsilon_1 = 0.01, \quad \epsilon_2 = 0.01, \quad \epsilon_3 = 0.01,\\
&\varepsilon_1 = 0.01, \quad \varepsilon_2 = 0.01, \quad \varepsilon_3 = 0.01,\\
&\eta_1 = 20, \quad \eta_2 = 2, \quad \eta_3 = 2,\\
&\alpha_1 = 10, \quad \alpha_2 = 2, \quad \alpha_3 = 2,\\
&b_1 = 1, \quad b_2 = 1\\
&k_1^P = 4, \quad k_1^D = 2, \quad k_1^I = 2, \quad \varGamma_1 = 4,\\
&k_2^P = 4, \quad k_2^D = 2, \quad k_2^I = 2, \quad \varGamma_i = 5,\\
&k_3^P = 15, \quad k_3^D = 10, \quad k_3^I = 10, \quad \varGamma_i = 1.
\end{aligned}$$

The proposed fuzzy adaptation range has been used for all adaptive gains in the design of the attitude controller. It has been also used in the estimation of $\hat{\tau}_{i,n}$ $(n = 1, 2, 3, 4)$ for the position control.

First, to show the effectiveness of the proposed controller for attitude control, the proposed controller is compared in two forms: adaptive integral backstepping terminal sliding mode (AIBTSMC) and adaptive backstepping sliding mode control (ABSMC). The transient behavior of attitude tracking error is shown in Fig. 3. It is obvious that proposed ABSMC method needs a longer time to reach a satisfactory tracking accuracy, but the proposed AIBTSMC

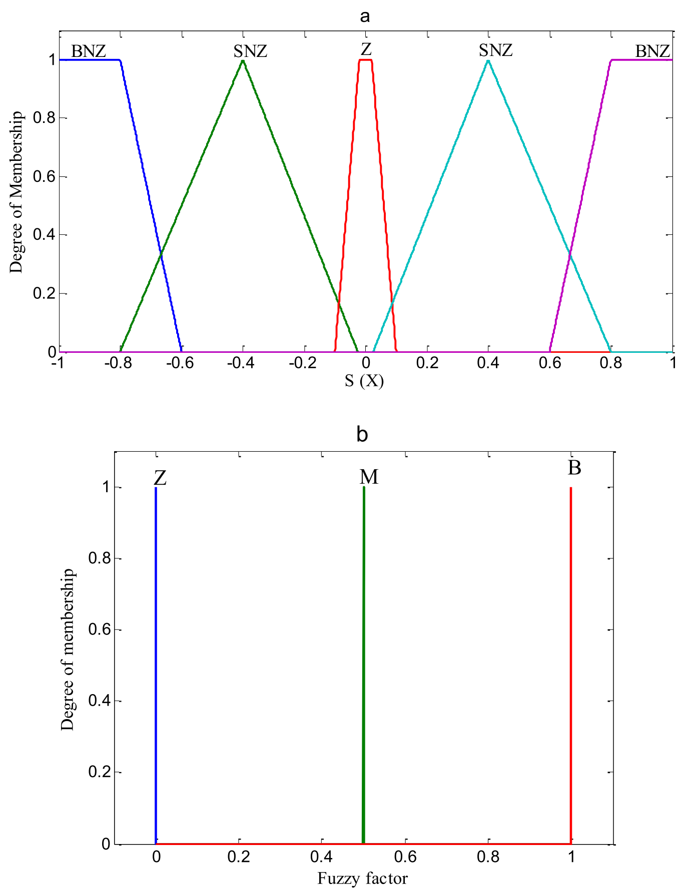


**Fig. 2.** Membership functions of (a) input, (b) output linguistic variables.

**Table 1**
Parameters of the quadrotor model.

| Parameter description | Parameter | Value |
|---|---|---|
| Mass of the quadrotor | $m$ | 0.6 (kg) |
| Distance between the mass center and rotors | $l$ | 0.23 (m) |
| Gravitational acceleration | $g$ | 9.81 $(\text{m/s}^2)$ |
| Moment of inertia around the $x$-axis | $I_x$ | 0.0075 $\text{kg m}^2$ |
| Moment of inertia around the $y$-axis | $I_y$ | 0.0075 $\text{kg m}^2$ |
| Moment of inertia around the $z$-axis | $I_z$ | 0.013 $\text{kg m}^2$ |
| Moment of inertia around the propeller axis | $J_p$ | 0.000065 $\text{kg m}^2$ |
| Drag coefficients for the translational dynamic | $K_{1,2,3}$ | 0.01 N/m |
| Drag coefficients for the rotational dynamic | $K_{4,5,6}$ | 0.005 N/m |

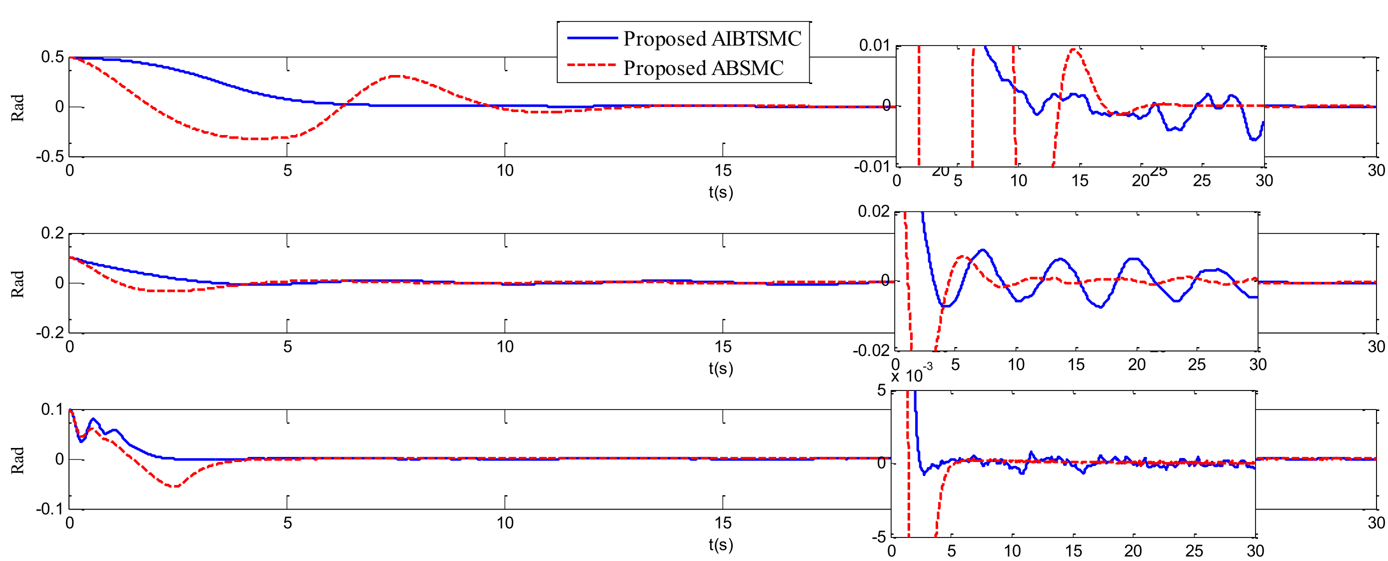


**Fig. 3.** Time responses of quadrotor attitudes in the presence of external disturbances.

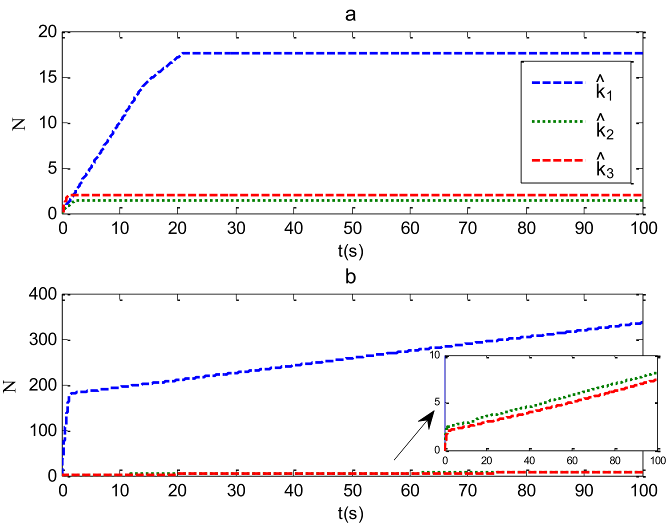


**Fig. 4.** Time response of the estimated gains $k_i$ for $i = 1, 2, 3$, respectively blue, green and red (a) with the proposed fuzzy adaptation range, (b) with the conventional adaptation law. (For interpretation of the references to color in this figure legend, the reader is referred to the web version of this article.)

can force the system trajectory to reach the sliding surface and assure tracking error convergence to zero in finite time with smaller variation and settling time. Thus, the tracking error is obtained by the proposed controller with integral state and terminal surface shows a more suitable tracking accuracy and transient behavior. Furthermore, using integral action in the controller design leads to zero steady state error but a greater overshoot.

Another comparison study has been shown in Fig. 4. This figure shows the different behavior of the modified estimation law and the conventional estimation for $k_i$ for $i = 1, 2, 3$. The proposed fuzzy adaptation range improves the estimation response and avoids the boundless increase.

In order to show the performance of full control of quadrotor with the two proposed controllers, another simulation example has been introduced: one simulation for attitude control and another one for position and altitude control. The reference trajectory is a circle evolving in the cartesian space defined as follows:

$$x_d = \cos(0.5t)\ \text{m}, \qquad y_d = \sin(0.5t)\ \text{m},$$

$$z_d = 1 + t\ \text{m}, \qquad \psi_d = 0\ \text{rad}$$

The quadrotor starts from $\xi_0 = [1.5, 0.5, 0]^T$ m and $\eta_0 = [0.1, 0.1, 0.1]^T$ rad. External disturbances exist and affect in both attitude and position dynamics of the quadrotor. These disturbances, including measurement noise on outputs and effects of wind disturbance, are considered in the first experiment as follows:

$$d_i = \sin(t) + 0.2\sin(100\pi t)\ \text{N}, \quad \text{for } i = 1, 2, 3.$$

$$W_i = 1\ \text{N}, \quad \text{for } i = 4, 5, 6, \text{ when } 15 \le t \le 50\ \text{s}.$$

The controller parameters are defined as before and are used in the simulations. Figs. 5 and 6 show the effectiveness of the proposed controllers, used for full control of the quadrotor in the presence of external disturbances. These figures show that the disturbances are compensated quickly and the desired tracking is achieved.

The desired pitch, roll and yaw angles, applied as virtual control signal (for the position control) which are obtained by the proposed adaptive PID, are shown in Fig. 7. It can be seen that the control inputs are smooth and free of any chattering.

The control signals of the quadrotor are shown in Fig. 8. The control inputs are smooth and the chattering phenomena is de-

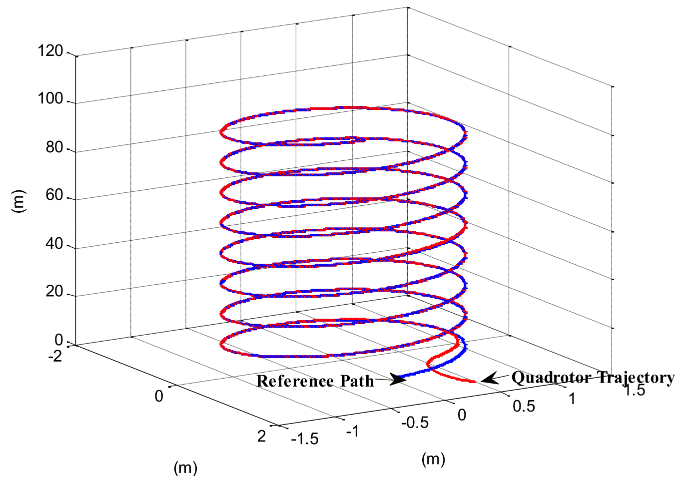


**Fig. 5.** 3D path tracking of the quadrotor with the proposed control scheme for attitude and position control in the presence of external disturbances in the both loops.

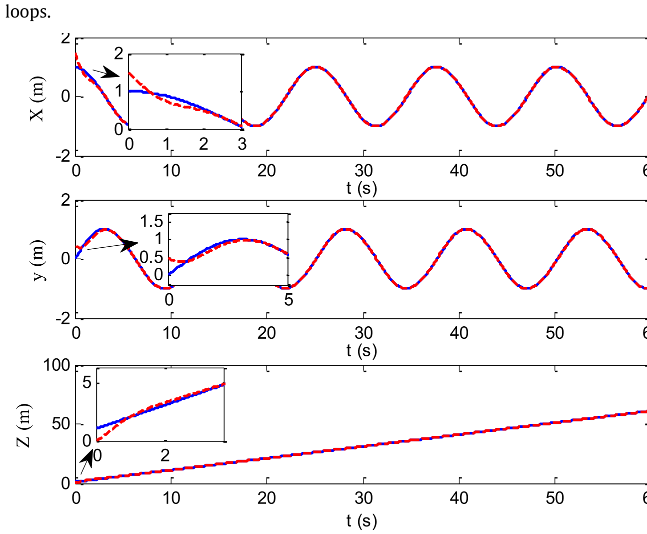


**Fig. 6.** Positions $(x, y, z)$ with external disturbances in the first experiment.

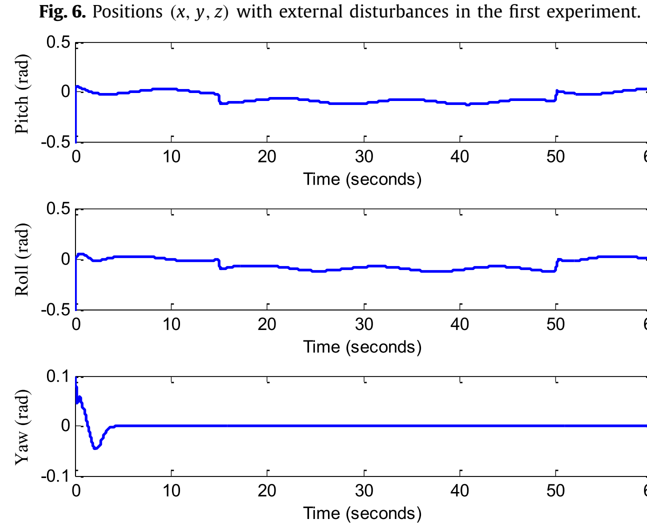


**Fig. 7.** Time responses of the desired pitch, roll and yaw angles in the first experiment.

creased using the proposed controller. The amplitudes of the control inputs are also practically realizable and small. The effect of disturbances and the controller compensation action are shown in Fig. 8.

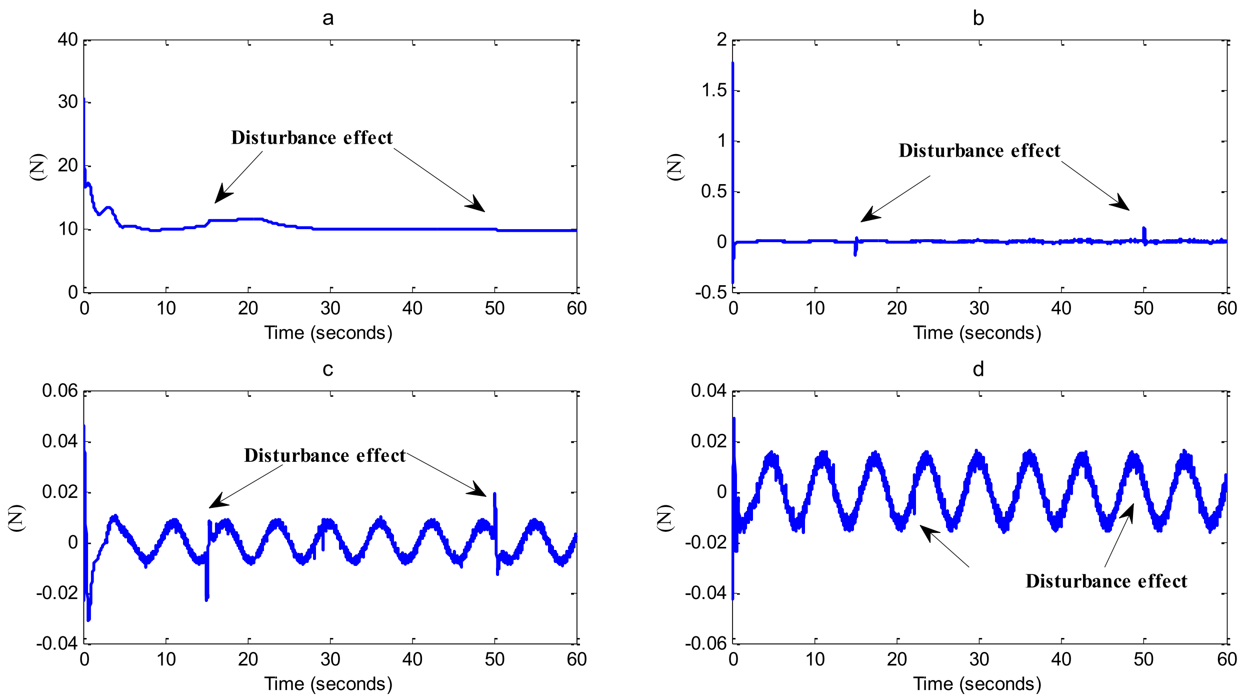


**Fig. 8.** The control inputs with external disturbances, (a) $u_1$, (b) $\tau_1$, (c) $\tau_2$, (d) $\tau_3$ in the first experiment.

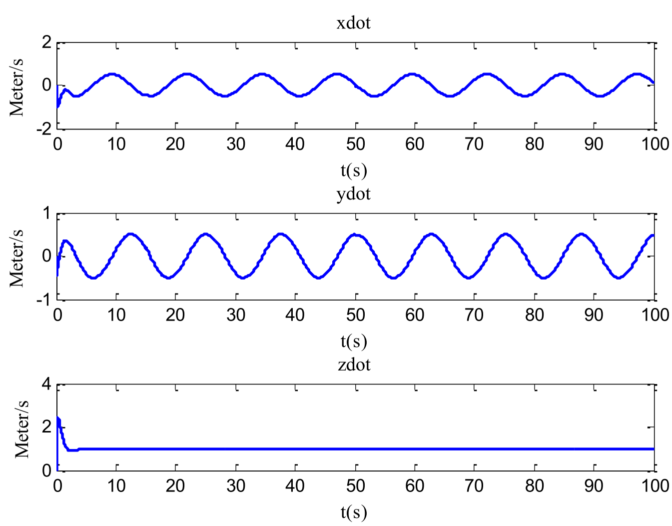


**Fig. 9.** Time response of linear velocity in the presence of external disturbances.

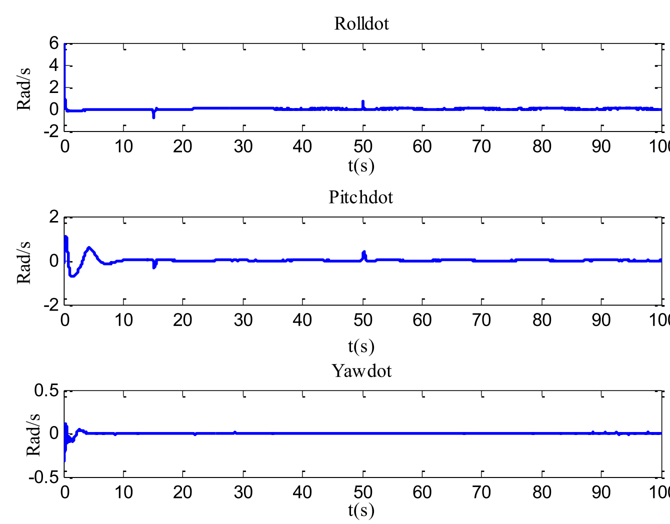


**Fig. 10.** Time response of angular velocity in the presence of external disturbances.

Figs. 9 and 10 show the effects of the proposed controllers in the tracking response of linear and angular velocities. It can be seen clearly that the effects of external disturbances have been compensated via the proposed attitude control scheme.

The estimated parameters of the proposed controller for the quadrotor attitude have been shown before. Fig. 11 shows the performance of adaptation gains for the proposed position controller in the presence of external disturbances. Moreover, the estimated value of the proposed controller for altitude control is shown in Fig. 12. The initial vector of the parameters is defined as follows:

$$\hat{\tau}_{4,n} = [15, 15, 15, 15], \qquad \hat{\tau}_{5,n} = [20, 20, 20, 20],$$

$$\hat{\tau}_{6,n} = [15, 25, 10, 5]\ (\mathrm{N})$$

In order to evaluate the performance of the controller, another simulation with a stricter situation has been provided and some new results are shown and analyzed. The wind disturbances effect is introduced as follows in this experiment

$$W_i(t) = \begin{cases} 0, \quad 0 \le t \le 15 \\ 0.8\sin(\frac{\pi(t-30)}{31}) + 0.4\sin(\frac{\pi(t-30)}{7}) \\ \quad + 0.08\sin(\frac{\pi(t-30)}{2}) \\ \quad + 0.056\sin(\frac{\pi(t-30)}{11}), \quad 15 < t \le 45 \\ 0, \quad 45 < t \le 65 \\ 0.8\sin(\frac{\pi(t-65)}{31}) + 0.4\sin(\frac{\pi(t-65)}{7}) \\ \quad + 0.08\sin(\frac{\pi(t-65)}{2}) \\ \quad + 0.056\sin(\frac{\pi(t-65)}{11}), \quad 65 < t \le 85 \\ 0, \quad 85 < t \le 100 \end{cases}$$

This disturbance has a time varying value limited to $\pm 1.826$ and it has been depicted in Fig. 13. Similar design parameters and $d_i$ have been considered for the second experiment.

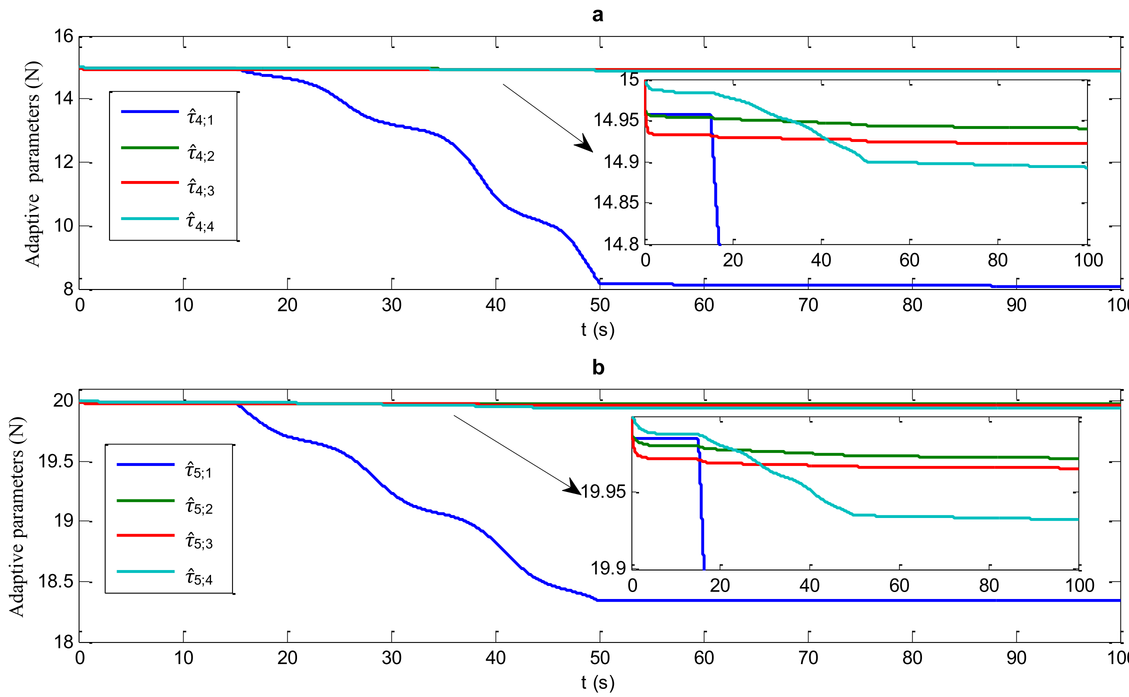


**Fig. 11.** The estimated parameters (a) $\hat{\tau}_{4,n}$, $n = 1, 2, 3, 4$, (b) $\hat{\tau}_{5,n}$, $n = 1, 2, 3, 4$.

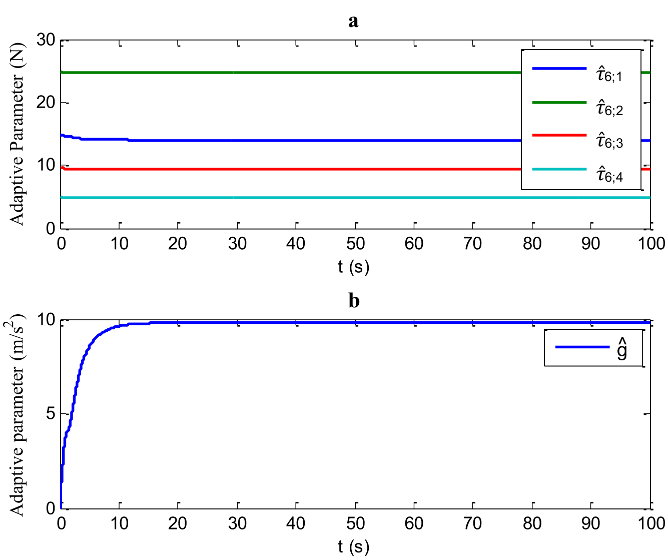


**Fig. 12.** The estimated parameters (a) $\hat{\tau}_{6,n}$, $n = 1, 2, 3, 4$ respectively and (b) $\hat{g}$.

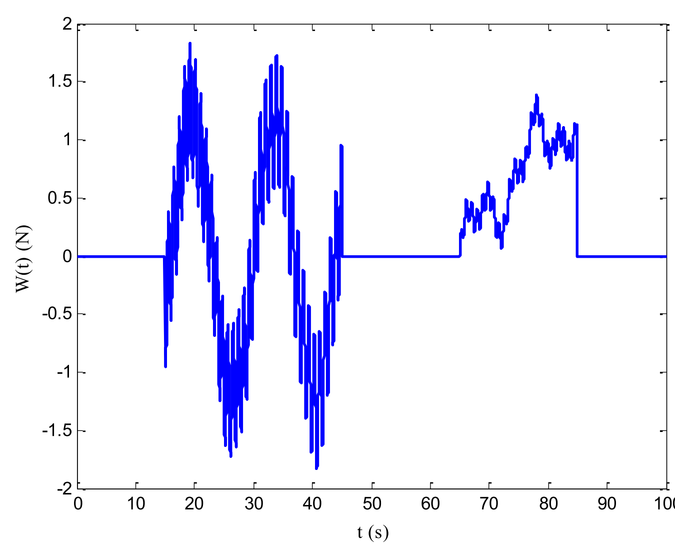


**Fig. 13.** The wind effect in the second experiment.

Since the densities of materials are not precise and they can change by motors or other elements, the values of inertia elements can be influenced and cause some uncertainties. In this experiment, some underrated model uncertainties have been considered in $b$, $d$ and the inertia matrices are as

$$\tilde{b} = 0.75b, \qquad \tilde{d} = 0.73d, \qquad \tilde{I}_x = 0.75I_x,$$
$$\tilde{I}_y = 0.75I_y, \qquad \tilde{I}_z = 0.65I_z.$$

The position states usually have been measured with GPS sensor or vision sensors and it can be modified by a barometer or magnetometer, but in these cases the noise is always a problem. The angular states have often been measured by IMU or Gyroscope. Depending on the precision of the sensors, big or small noise can be occurred. Therefore, a 50% random noise has been applied for all the states as follows

$$\tilde{x} = x.(rand + 0.5)$$

where *rand* is a random function with the output range between 0 and 1.

As it can be seen in Figs. 14, 15 and 16, the disturbances effect, model uncertainty and measurement noise have been compensated during the scenario with the proposed controller. The wind effect has been applied and it has been rejected by the robust action of the controller. Noise and uncertainties on model have also had negative effect on the system, but their bad effects have been reduced through the proposed controller.

## 8. Conclusion

In this paper, a novel hybrid nonlinear control schemes have been proposed for quadrotor attitude, altitude and position control.

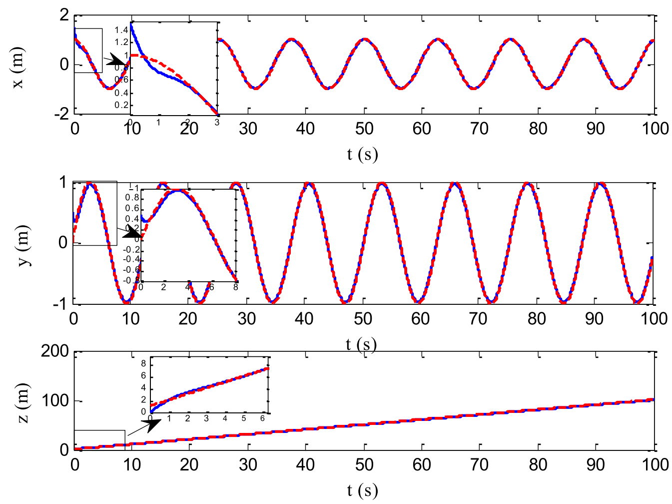


**Fig. 14.** Positions $(x, y, z)$ in the second experiment.

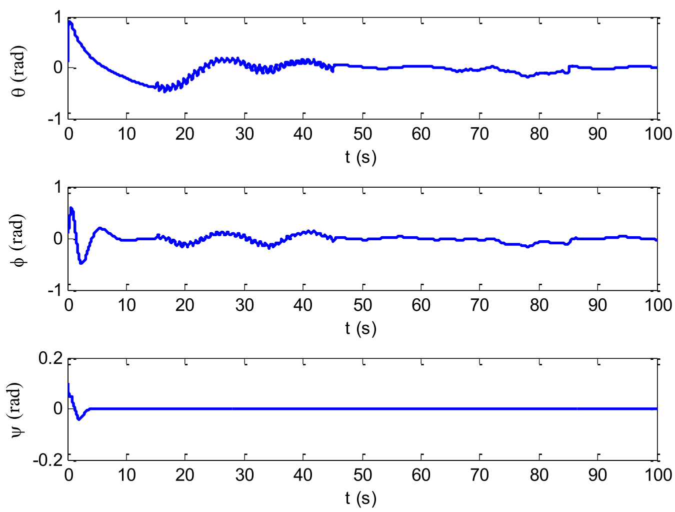


**Fig. 15.** Time responses of the desired pitch, roll and yaw in the second experiment.

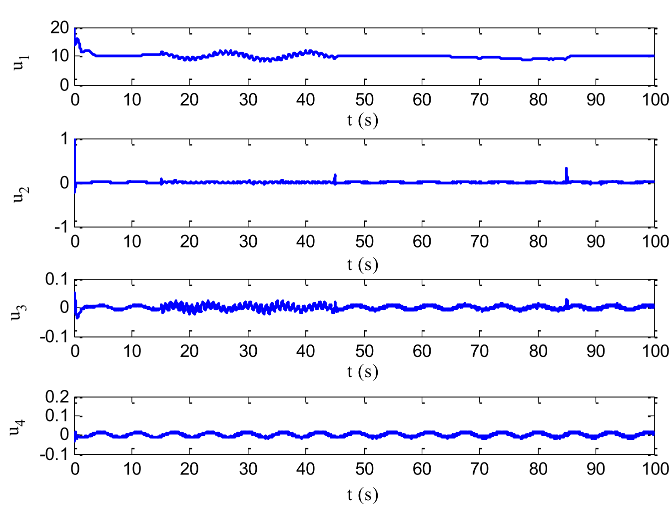


**Fig. 16.** Control inputs with external disturbances, (a) $u_1$, (b) $\tau_1$, (c) $\tau_2$, (d) $\tau_3$ in the second experiment.

Euler angles have been stabilized with a novel finite time approach based on the combination of integral backstepping method and adaptive terminal sliding mode control. The position controller has been designed based on free chattering robust adaptive PID control. Unknown bounds of limited disturbance have been estimated via adaptive control with novel fuzzy adaptive range to avoid over-estimation. Transient and steady state behaviors of tracking error have been improved using these control schemes.

The proposed controller demonstrates robustness and improves the transient response of the system's output against harsh wind disturbances and uncertainties. The control signal variations have been decreased efficiently. MATLAB software and SIMULINK environment have been used to validate this study. A comparison study has been carried out to show the advantages of the modified adaptive range and the attitude control scheme. The simulations show also appropriate path following in the presence of external disturbances.

## Conflict of interest statement

The authors certify that they have no affiliations with or involvement in any organization or entity with any financial interest or non-financial interest in the subject matter or materials discussed in this manuscript.

## Appendix A. Supplementary material

Supplementary material related to this article can be found online at http://dx.doi.org/10.1016/j.ast.2015.05.022.

## References

[1] F. Lewis, Dynamic inversion with zero-dynamics stabilisation for quadrotor control, IET Control Theory Appl. 3 (3) (2009) 303–314.
[2] S. Bouabdallah, R. Siegwart, Backstepping and sliding-mode techniques applied to an indoor micro quadrotor, in: Proc. of the IEEE International Conference on Robotics and Automation, Barcelona, Spain, April 2005, pp. 2247–2252.
[3] T. Madani, A. Benallegue, Backstepping control for a quadrotor helicopter, in: The 2006 IEEE/RSJ International Conference on Intelligent Robots and Systems, China, 2006, pp. 3255–3260.
[4] M. Bouchoucha, S. Seghour, H. Osmani, M. Bouri, Integral backstepping for attitude tracking of a quadrotor system, Elektron. Elektrotech. 116 (10) (2011).
[5] Z. Fang, W. Gao, Adaptive integral backstepping control of a Micro-Quadrotor, in: The 2nd International Conference on Intelligent Control and Information Processing, Harbin, July 2011, pp. 910–915.
[6] H. Bouadi, M. Bouchoucha, M. Tadjine, Modelling and stabilizing control laws design based on sliding mode for an UAV type-quadrotor, Eng. Lett. 15 (2) (2007) 342.
[7] R. Xu, Ü. Özgüner, Sliding mode control of a quadrotor helicopter, in: 45th IEEE Conference on Decision & Control, USA, 2006, pp. 4957–4962.
[8] L. Besnarda, Y.B. Shtessel, B. Landrum, Quadrotor vehicle control via sliding mode controller driven by sliding mode disturbance observer, J. Franklin Inst. 349 (2) (2012) 658–684.
[9] L. Derafa, A. Benallegue, L. Fridman, Super twisting control algorithm for the attitude tracking of a four rotors UAV, J. Franklin Inst. 349 (2) (2012) 685–699.
[10] D. Lee, H.J. Kim, S. Sastry, Feedback linearization vs. adaptive sliding mode control for a quadrotor helicopter, Int. J. Control. Autom. Syst. 7 (3) (2009) 419–428.
[11] H. Yu, J. Wang, B. Deng, X. Wei, Y. Che, Y.K. Wong, W.L. Chan, K.M. Tsang, Adaptive backstepping sliding mode control for chaos synchronization of two coupled neurons in the external electrical simulation, Commun. Nonlinear Sci. Numer. Simul. 17 (3) (2012) 1344–1354.
[12] N. Chen, F. Song, G. Li, X. Sun, Ch. Ai, An adaptive sliding mode backstepping control for the mobile manipulator with nonholonomic constraints, Commun. Nonlinear Sci. Numer. Simul. 18 (10) (2013) 2885–2899.
[13] A. Tayebi, S. McGilvray, Attitude stabilization of a four-rotor aerial robot, in: Proc. of the IEEE Conference on Decision and Control, Atlantis, Paradise Island, Bahamas, Dec. 2004, pp. 1216–1221.
[14] A. Tayebi, S. McGilvray, Attitude stabilization of a VTOL quadrotor aircraft, IEEE Trans. Control Syst. Technol. 14 (3) (2006) 562–571.
[15] C. Nicol, C.J.B. Macnab, A. Ramirez-Serrano, Robust adaptive control of quadrotor helicopter, Mechatronics 21 (6) (2011) 927–938.

[16] Z.T. Dydek, Anuradha M. Annsawany, Eugene Lavretsky, Adaptive control of quadrotor UAVs: a design trade study with flight evaluations, IEEE Trans. Control Syst. Technol. 21 (4) (2012) 1400–1406.

[17] J. Xu, L. Qiao, Robust adaptive PID control of robot manipulator with bounded disturbances, Math. Probl. Eng. 2013 (2013), Article ID 535437, 13 pages, http://dx.doi.org/10.1155/2013/535437.

[18] J.-J. Xiong, E.-H. Zheng, Position and attitude tracking control for a quadrotor UAV, ISA Trans. 53 (3) (2014) 725–731.

[19] H. Wang, Z. Han, Q. Xie, W. Zhang, Finite-time chaos synchronization of unified chaotic system with uncertain parameters, Commun. Nonlinear Sci. Numer. Simul. 14 (5) (2009) 2239–2247.

[20] S.P. Bhat, D.S. Bernstein, Finite-time stability of continuous autonomous systems, SIAM J. Control Optim. 38 (3) (2000) 751–766.

[21] M.P. Aghababa, M.E. Akbari, A chattering-free robust adaptive sliding mode controller for synchronization of two different chaotic systems with unknown uncertainties and external disturbances, Appl. Math. Comput. 218 (2012) 5757–5768.

[22] S. Mondal, C. Mahanta, Chattering free adaptive multivariable sliding mode controller for system with matched and mismatched uncertainty, ISA Trans. 52 (3) (2013) 335–341.

[23] E. Slotine, W. Li, Applied Nonlinear Control, 1st ed., Prentice–Hall, 1991.

[24] H. Xu, M. Mirmirani, Adaptive sliding mode control design for a hypersonic flight vehicle, J. Guid. Control Dyn. 27 (5) (2004) 829–838.

[25] S. Yu, X. Yu, B. Shirinzadeh, Continuous finite time control for robotic manipulators with terminal sliding mode, Automatica 41 (11) (2005) 1957–1964.

[26] D. Zhao, S. Li, F. Gao, A new terminal sliding mode control for robotic manipulators, Int. J. Control 82 (10) (2009) 1804–1813.

[27] R. Zhang, C. Sun, J. Zhang, Y. Zhou, Second-order terminal sliding mode control for hypersonic vehicle in cruising flight with sliding mode disturbance observer, J. Control Theory Appl. 11 (2) (2013) 299–305.

[28] F. Plestan, Y. Shtessel, V. Bregeault, A. Poznyak, New methodologies for adaptive sliding mode control, Int. J. Control 9 (9) (2011) 1907–1919.

[29] W. Xiang, F. Chen, Coplement to 'Second-order terminal sliding mode controller for a class of chaotic systems with unmatched uncertainties' [Commun. Nonlinear Sci. Numer. Simul. 15 (2010) 3241–3247], Commun. Nonlinear Sci. Numer. Simul. 16 (6) (2011) 2658–2661.

[30] M. Zhihong, X.H. Yu, Terminal sliding mode control of MIMO linear systems, in: Proceedings of the 35th IEEE Conference on Decision and Control, 1996, pp. 4619–4624.

[31] Y. Feng, X. Yu, Z. Man, Non-singular terminal sliding mode control of rigid manipulators, Automatica 38 (2002) 2159–2167.

[32] Y. Feng, X. Yu, F. Han, On nonsingular terminal sliding-mode control of nonlinear systems, Automatica 49 (2013) 1715–1722.